

Clustering in the Skyrme-Force Hartree-Fock Approach

GEFÖRDERT VOM



Bundesministerium
für Bildung
und Forschung

Collaborators

P.-G. Reinhard, U. Erlangen

N. Itagaki, Kyoto

T. Ichikawa, Kyoto

S. Umar, Vanderbilt U.

Lu Guo, Tokyo U.

H. Horiuchi, RCNP Osaka

V. Oberacker, Vanderbilt U.

N. Löbl, U. Frankfurt

M. Kimura, Sapporo

S. Schramm, U. Frankfurt

P. Stevenson, Surrey

B. Schuetrumpf, Frankfurt

Initial Publications

- J. A. Maruhn, M. Kimura, S. Schramm, P.-G. Reinhard, H. Horiuchi, and A. Tohsaki, "Alpha Cluster Structure and Exotic States in a Self-Consistent Model for Light Nuclei", *Phys. Rev. C* **74**, 044311 (2006).
- J.A. Maruhn, N. Loeb, N. Itagaki, and M. Kimura, "Linear-chain structure of three α -clusters in ^{16}C and ^{20}C ", *Nucl. Phys. A* **833**, 1 (2010).
- A. S. Umar, J. A. Maruhn, N. Itagaki, and V. E. Oberacker, "Microscopic Study of the Triple- α Reaction", *Phys. Rev. Lett.* **104**, 212503 (2010).
- 板垣直之, Joachim A. Maruhn, and 木村真明, "中性子の果たす"糊"の効果と α クラスターの結合形態", *日本物理学会誌* **64**, 840 (2009).
- Methods
 - Static and time-dependent Hartree-Fock
 - Full Skyrme force
 - Cartesian grid in 3D, no symmetries
 - Differencing using FFT
 - Exact treatment of Coulomb boundary condition

Alpha Cluster Structure and Exotic States in a Self-Consistent Model for Light Nuclei

- Search for presence of α -clustering in pure mean-field states (no projection): result is a Slater determinant defined by occupied s.p. wave functions given on a 3D Cartesian grid
- Despite the „independent particle model“, correlations are present through the mean field, which can produce similar wave functions for quartets
- The existence of clusters is not assumed in the theory

Cluster Analyses

- The result is always the overlap of two many-body wave functions, leading to determinants
- Pure a configurations: Gaussian wave functions distributed in
 - Prescribed geometry with scales adjustable
 - Fully free positioning; all position vectors fitted
- The radius parameter of the α 's was adjusted in the same way, in most cases all α 's had the same radius
- Numerically, a multidimensional optimization algorithm was used and proved very successful

Alternative Analyses

- Use a mixture of ground-state nuclei from a static HF calculation and /or α -clusters
- Expand over a number of similar configurations in a GCM manner
- In all cases the occupied states in the model state are partially non-orthogonal

General Properties

- Resulting static states were always axially and mirror-symmetric.
- δ -force pairing included, but was found to vanish in converged configurations

Localization Analysis

- Originally from molecular physics

*A. D. Becke and K. E. Edgecombe, J. Chem. Phys. **92**, 5397 (1990)*

- Definition actually used from

*T. Burnus, M.A.L. Marques, and E.K.U. Gross,
Phys. Rev. A **71**, 010501 (2005).*

- Applied to present study in:

*P.G. Reinhard, J. A. Maruhn, A.S. Umar, and V.E. Oberacker,
Phys. Rev. C **83**, 034312 (2011)*

- Localization is defined by having a particle at some position with low probability of finding another particle **of the same spin and isospin** nearby
- Probability of finding such a pair of nucleons at \mathbf{r} and \mathbf{r}' :

$$P_{q,\sigma}(\vec{r},\vec{r}') = \rho_{q,\sigma}(\vec{r})\rho_{q,\sigma}(\vec{r}') - \left| \rho_{qq\sigma\sigma}(\vec{r},\vec{r}') \right|^2$$

for same isospin q and spin σ .

The Localization Field

- Averaging over a spherical shell of radius δ and using a Taylor expansion we get

$$R_{q,\sigma}(\vec{r}, \delta) \approx \frac{\delta^2}{3} \left(\tau_{q,\sigma} - \frac{1}{4} \frac{|\nabla \rho_{q,\sigma}|^2}{\rho_{q,\sigma}} - \frac{\vec{j}_{q,\sigma}^2}{\rho_{q,\sigma}} \right)$$

with

$$\vec{j}_{q,\sigma}(\vec{r}) = \sum_{\alpha \in q} \text{Im}[\phi_{\alpha}^*(\vec{r}, \sigma) \nabla \phi_{\alpha}(\vec{r}, \sigma)], \quad \tau_{q,\sigma} = \sum_{\alpha \in q} |\nabla \phi_{\alpha}(\vec{r}, \sigma)|^2,$$

$$\nabla \rho_{q,\sigma}(\vec{r}) = 2 \sum_{\alpha \in q} \text{Re}[\phi_{\alpha}^*(\vec{r}, \sigma) \nabla \phi_{\alpha}(\vec{r}, \sigma)]$$

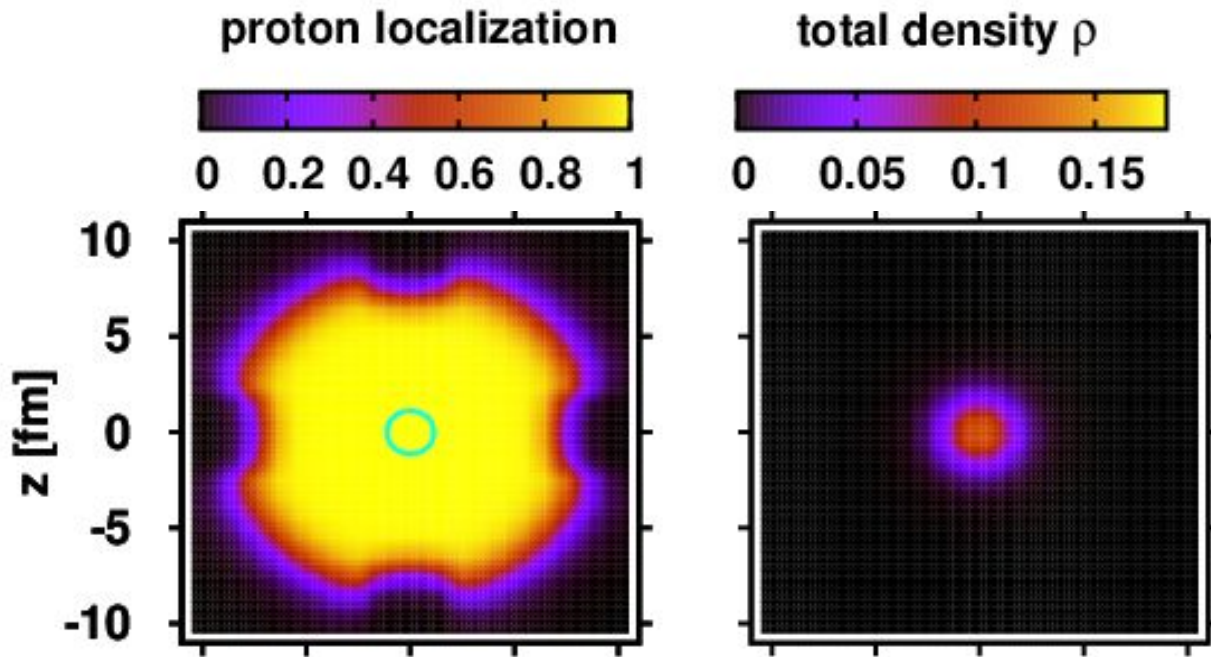
Since we want a measure for the absence of a second particle, we invert

$$R_{q,\sigma}(\vec{r}, \delta) \approx \left(1 + \left[\frac{\tau_{q,\sigma} \rho_{q,\sigma} - \frac{1}{4} |\nabla \rho_{q,\sigma}|^2 - \vec{j}_{q,\sigma}^2}{\rho_{q,\sigma} \tau_{q,\sigma}^{TF}} \right] \right)^{-1} \quad \text{with} \quad \tau_{q,\sigma}^{TF} = \frac{3}{5} (6\pi^2)^{2/3} \rho_{q,\sigma}^{5/3}$$

This is normalized to the range 0...1

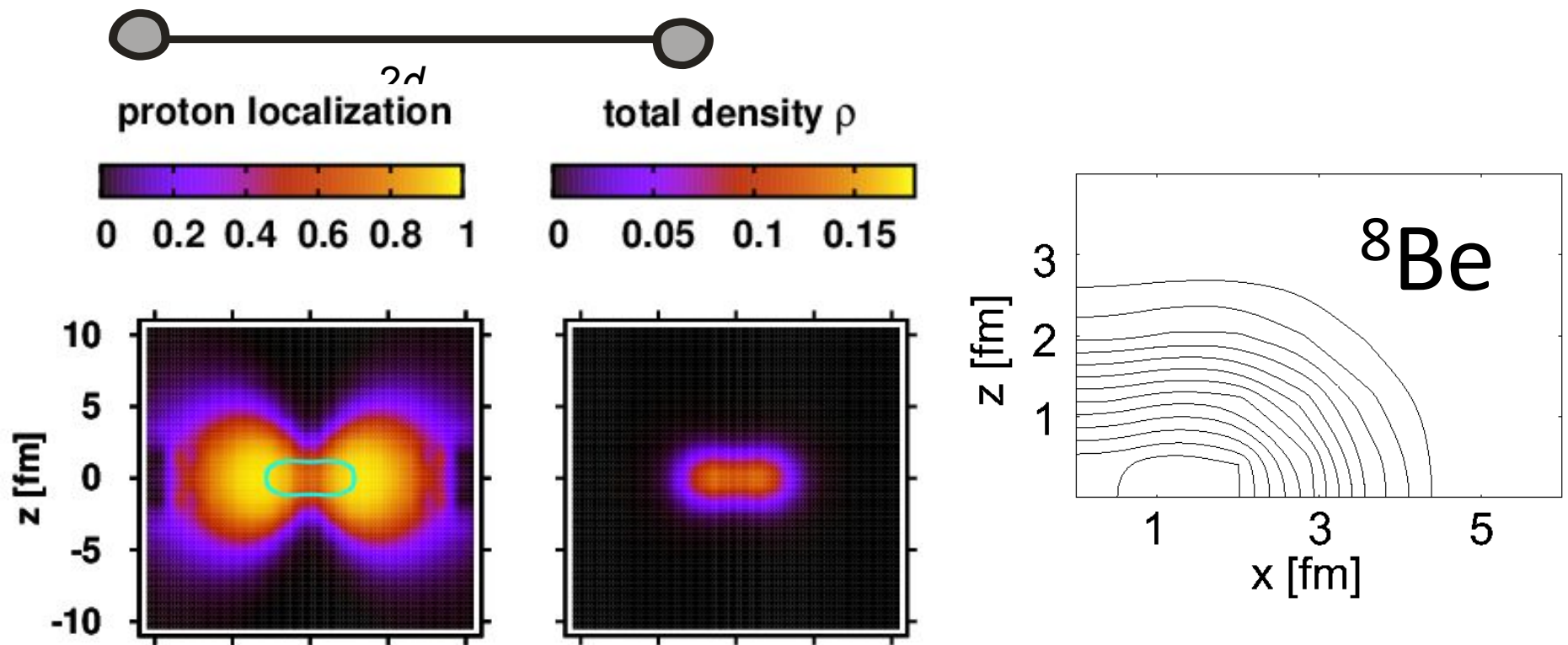
Limiting Cases

- For Fermi gas $R_{q,\sigma} \approx 1/2$ since $\tau \approx \tau^{TF}$
- For an α -particle, $R_{q,\sigma} \approx 1$, i. e. perfect localization



Numerical results for the localization are not meaningful in low-density regions

Force	E_{ls} [MeV]	β_2	Q_{20} [fm ²]	Cluster Analysis			α -GCM	
				\mathcal{O} [%]	d [fm]	σ [fm]	\mathcal{O} [%]	σ [fm]
SkI3	2.5	0.677	46.8	82	2.70	1.68	98	1.65
SkI4	2.7	0.669	46.2	81	2.64	1.69	97	1.64
Sly6	2.4	0.666	48.0	81	2.68	1.73	97	1.68
SkM*	4.6	0.593	38.0	71	2.20	1.68	82	1.62
NL3		0.679	40.7	85	2.52	1.56		
χ_m		0.671	41.8	68	2.60	1.60		



The Case of ^{12}C

Force	E_{ls} [MeV]	β_2	Q_{20} [fm ²]	Cluster Analysis	
				\mathcal{O} [%]	σ
SkI3	15.8	-0.256	-24.7	28	1.72
SkI4	21.6	0.000	0.00	1	1.66
Sly6	19.8	0.000	0.00	1	1.68
SkM*	23.6	0.000	0.00	1	1.64
NL3		0.000	0.00	1	1.48
χ_m		0.129	11.4	2	1.64

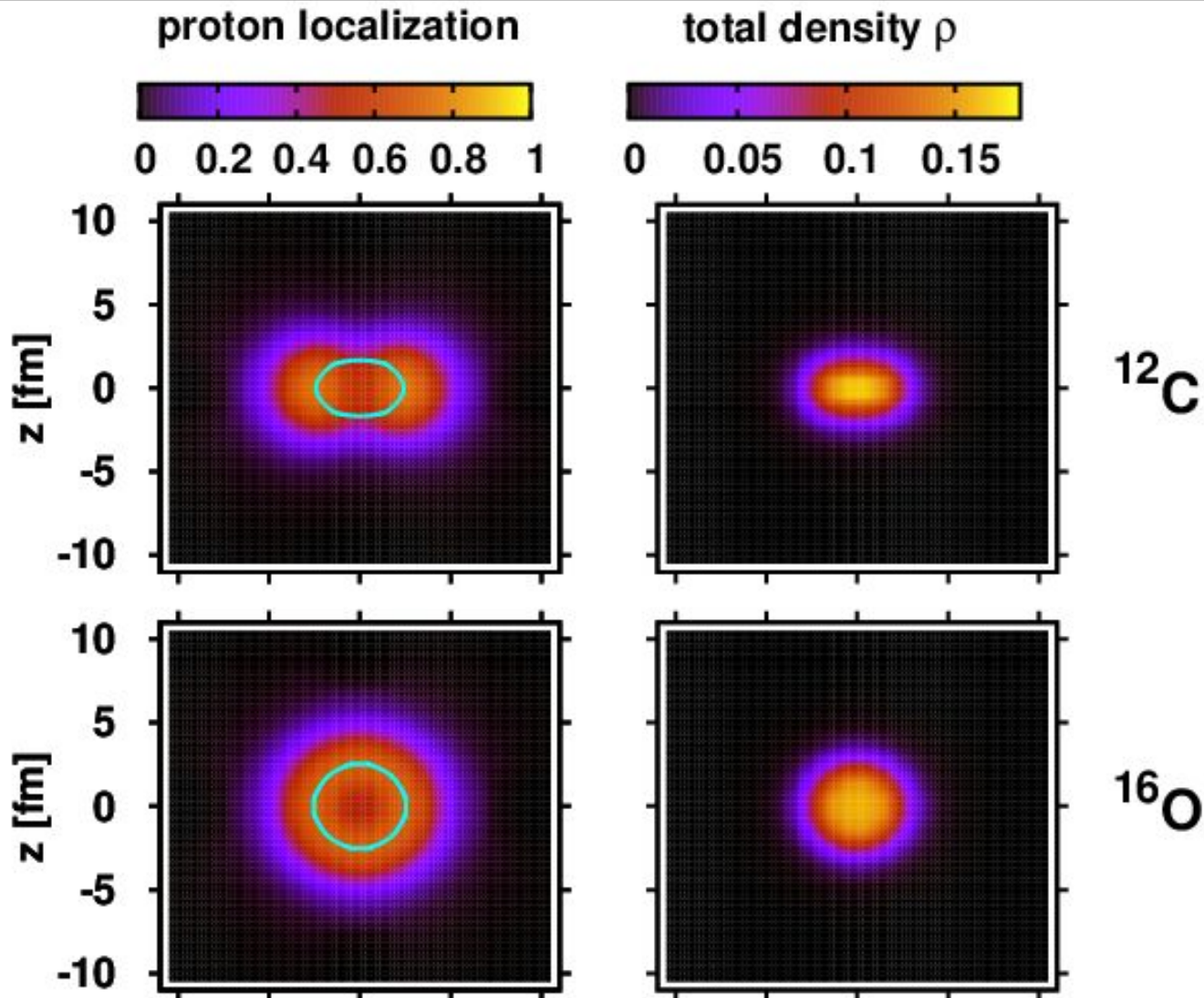
$l * s$ Reduction Factor	SkI3		Sly6	
	β_2	\mathcal{O} [%]	β_2	\mathcal{O} [%]
1.0	-0.256	28	0.00	1.68
0.8	-0.326	53	-0.017	1.97
0.6	-0.356	68	-0.303	46
0.4	-0.371	77	-0.337	62
0.2	-0.379	82	-0.356	72
0.0	-0.381	84	-0.367	79

The Case of ^{16}O

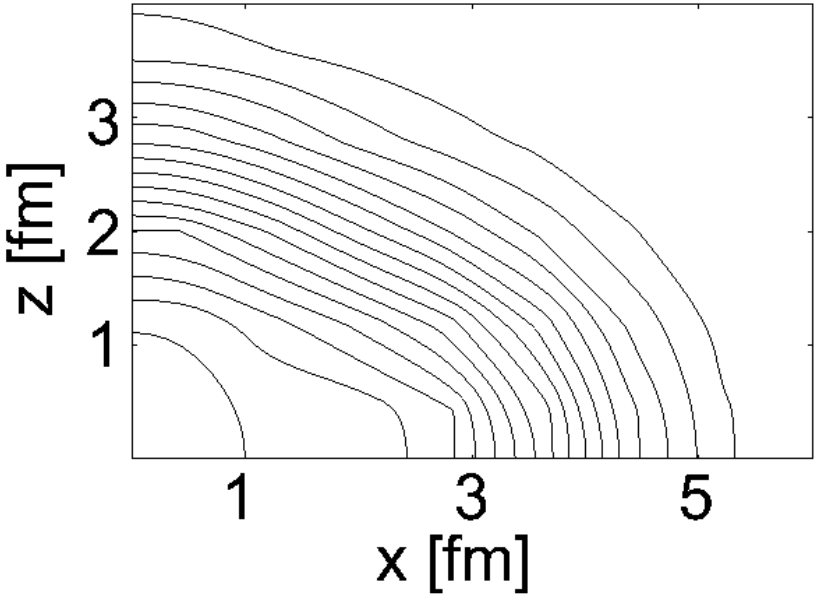
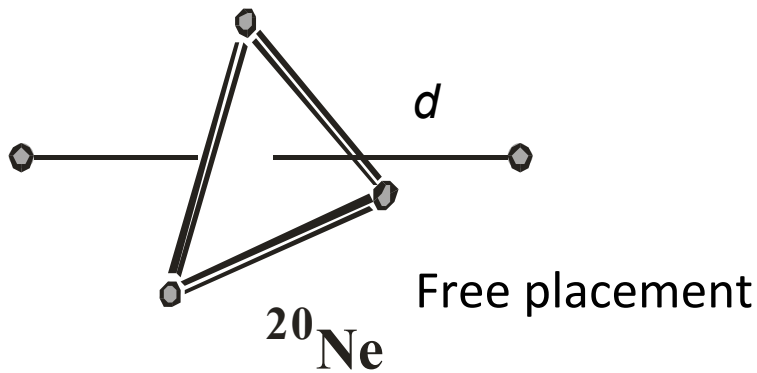
Force	E_{ls} [MeV]	R_{rms} [fm]	Cluster Analysis	
			\mathcal{O} [%]	σ [fm]
SkI3	1.0	2.65	96	1.76
SkI4	1.0	2.65	96	1.76
Sly6	0.9	2.69	96	1.79
SkM*	1.1	2.68	96	1.78
NL3		2.56	95	1.72
χ_m		2.58	79	1.71

- Four non-coplanar alpha-particles are required
- The precise arrangement is unimportant
- Their relative distance tends to zero
- This is not a cluster structure, but the close-lying Gaussians generate the p-states

Localization for ^{12}C and ^{16}O



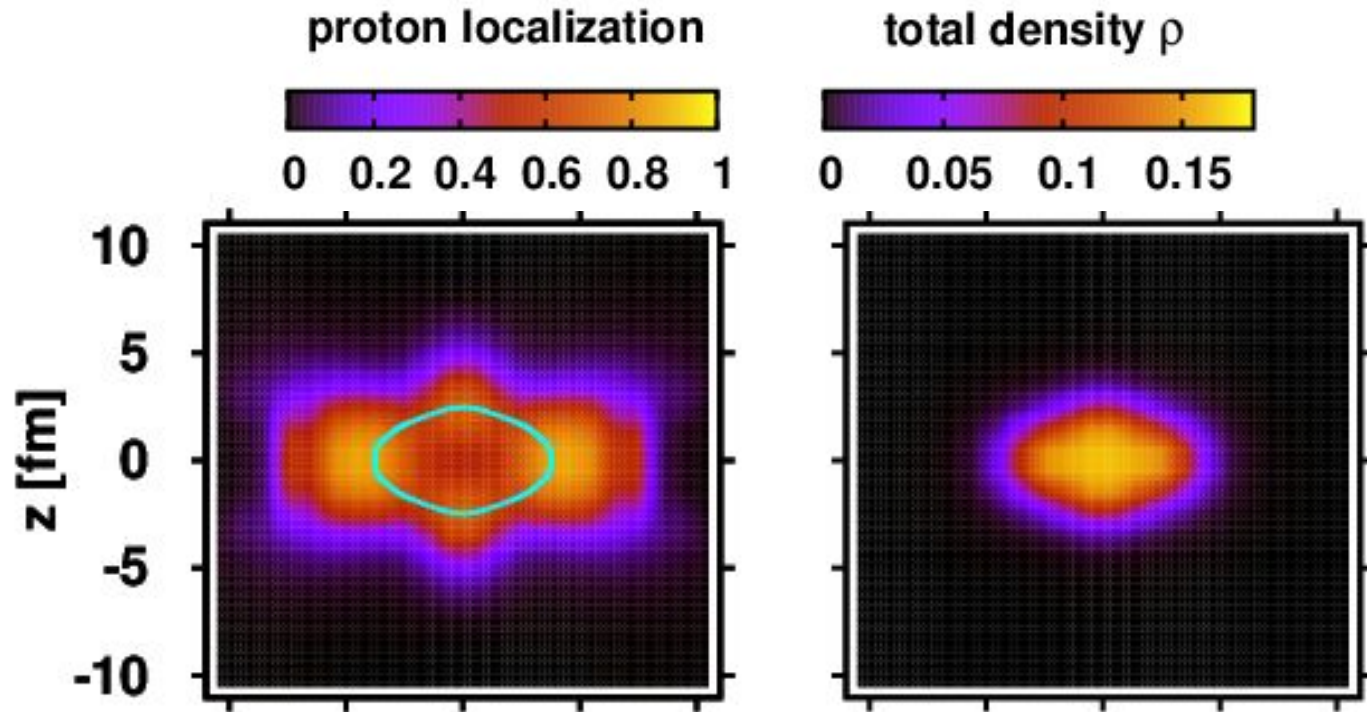
Force	E_{ls}	β_2	Q_{20}	Cluster Analysis			
	[MeV]		[fm ²]	\mathcal{O} [%]	d [fm]	σ_1 [fm]	σ_2 [fm]
SkI3	8.5	0.423	91.0	53	1.91	1.78	1.71
SkI4	9.2	0.412	88.0	49	1.86	1.78	1.71
Sly6	8.5	0.409	89.8	47	1.84	1.80	1.74
SkM*	11.1	0.371	79.2	36	1.59	1.77	1.73
NL3		0.425	84.4	59	1.83	1.74	1.65
χ_m		0.439	90.6	50	1.89	1.74	1.69



Force	$^{16}\text{O} + \text{static } \alpha$			$^{16}\text{O} + \alpha$ GCM	
	\mathcal{O} [%]	d [fm]	σ [fm]	\mathcal{O} [%]	σ [fm]
SkI3	52	2.7	1.59	54	1.56
SkI4	48	2.5	1.62	49	1.52
Sly6	48	2.6	1.66	49	1.55
SkM*	36	2.4	1.64	36	1.53

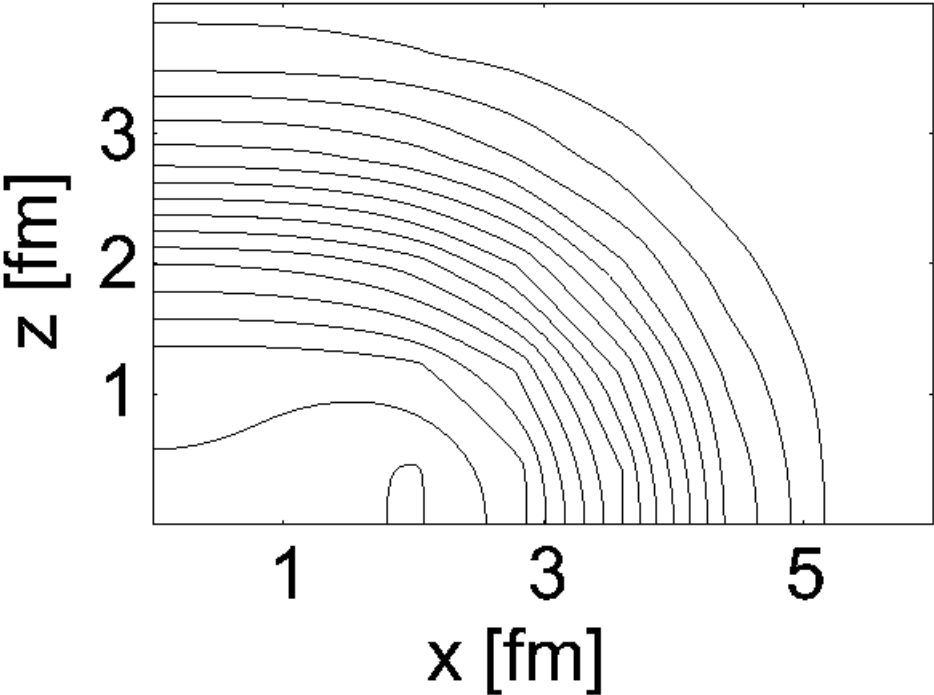
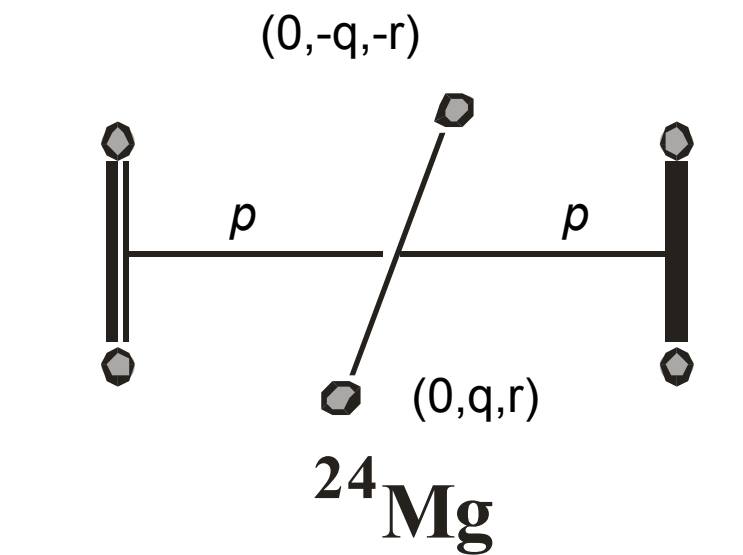
$^{16}\text{O} + \text{symmetrized } \alpha$

Localization for ^{20}Ne

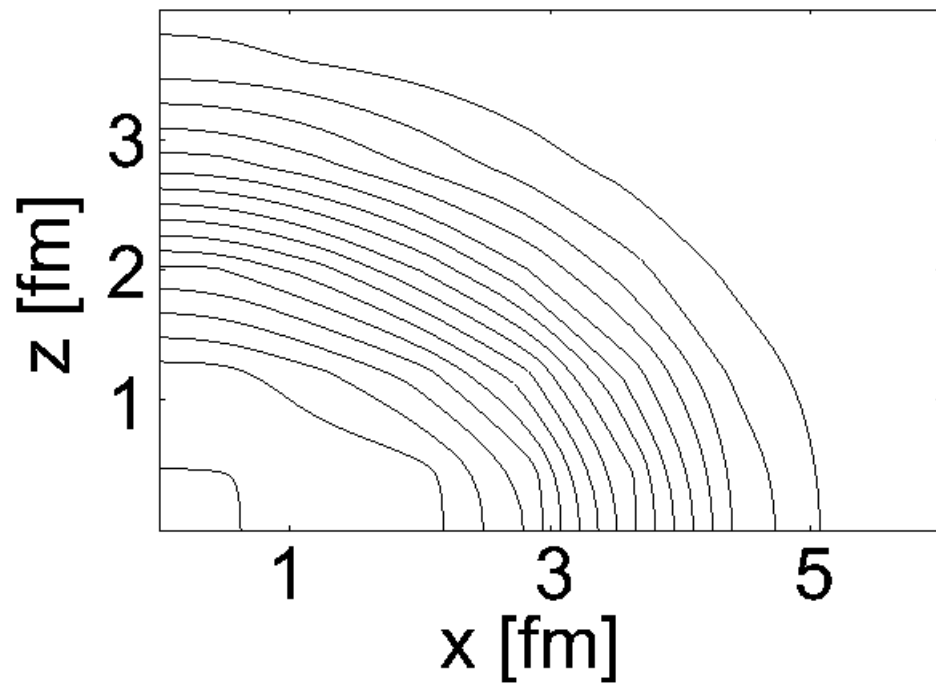
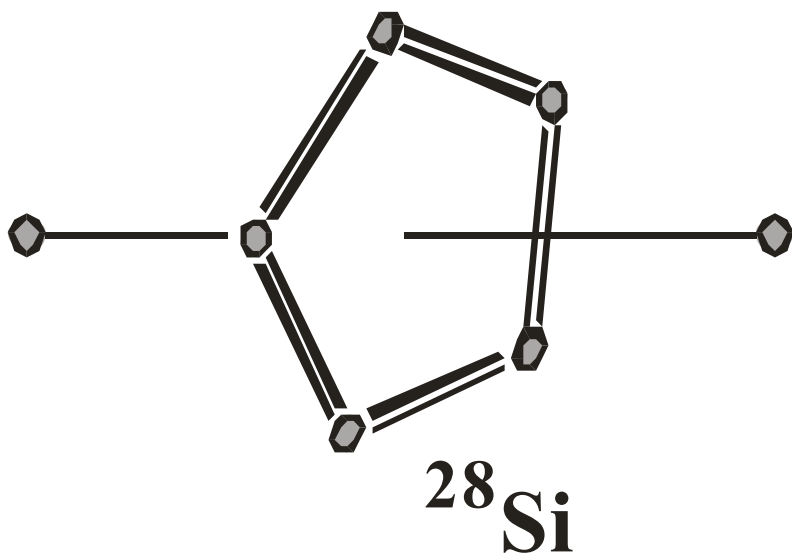


This supports the interpretation of a ^{12}C core with α -particles attached at the sides

Force	E_{ls} [MeV]	β_2	Q_{20} [fm ²]	Cluster Analysis				
				\mathcal{O} [%]	p [fm]	q [fm]	r [fm]	σ [fm]
SkI3	22.6	0.423	117.2	2.3	1.40	0.17	0.37	1.77
SkI4	23.5	0.416	114.1	2.2	1.38	0.10	0.41	1.76
Sly6	21.6	0.413	116.5	2.2	1.39	0.04	0.40	1.79
SkM*	25.4	0.389	107.0	1.8	1.31	0.15	0.41	1.77
NL3		0.416	103.9	2.0	1.37	0.17	0.45	1.71
χ_m		0.431	115.2	2.0	1.38	0.25	0.31	1.74

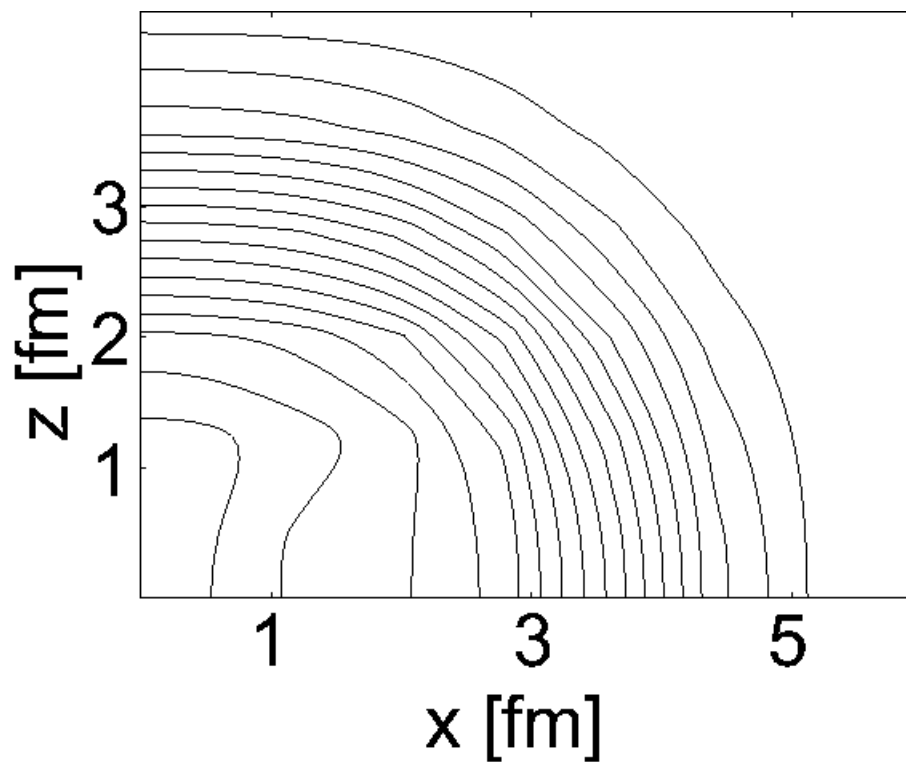


Force	E_{ls} [MeV]	β_2	Q_{20} [fm ²]	Cluster Analysis	
				\mathcal{O} [%]	σ [fm]
SkI3	30.2	-0.318	-108.5	7.8	1.86
SkI4	33.6	-0.294	-98.6	4.5	1.85
Sly6	31.7	-0.289	-98.8	4.0	1.87
SkM*	40.6	-0.224	-73.7	0.8	1.83
NL3		-0.303	-93.5	6.2	1.80
χ_m		-0.351	-117.9	14.9	1.85



Force	E_{ls} [MeV]	β_2	Q_{20} [fm ²]	Cluster Analysis	
				\mathcal{O} [%]	σ
SkI3	29.6	0.222	90.6	1.6	1.87
SkI4	37.0	0.147	58.7	0.3	1.86
Sly6	40.0	0.000	0.0	0.04	1.87
SkM*	44.7	0.000	0.0	0.03	1.86
NL3		0.228	86.24	1.8	1.83
χ_m		0.253	101.1	2.2	1.85

^{32}S

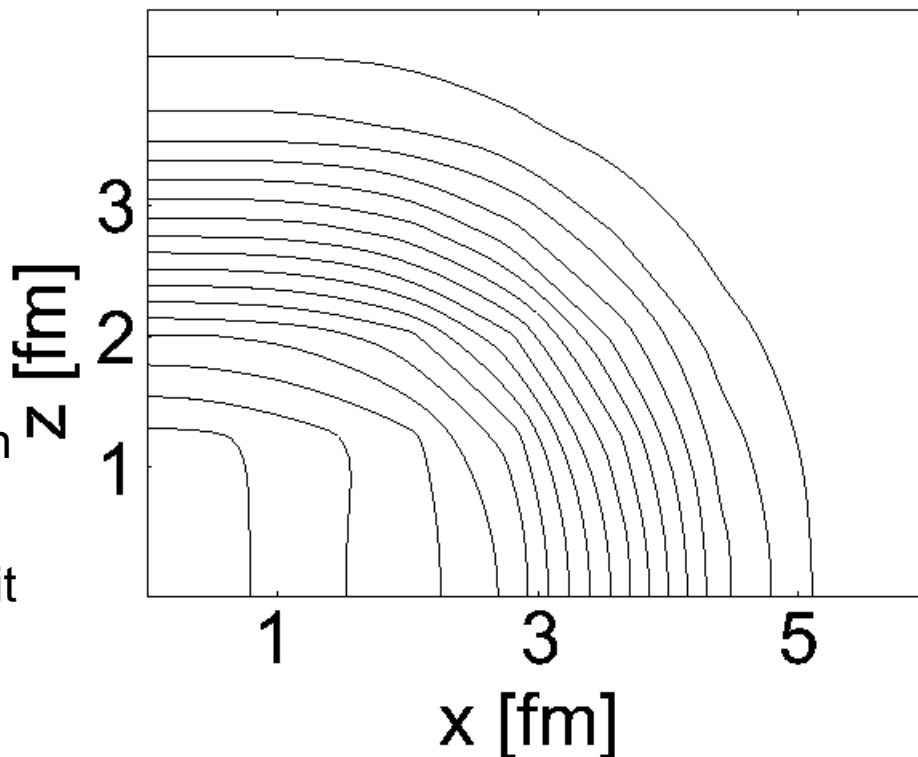


α 's closely concentrated
with random geometry

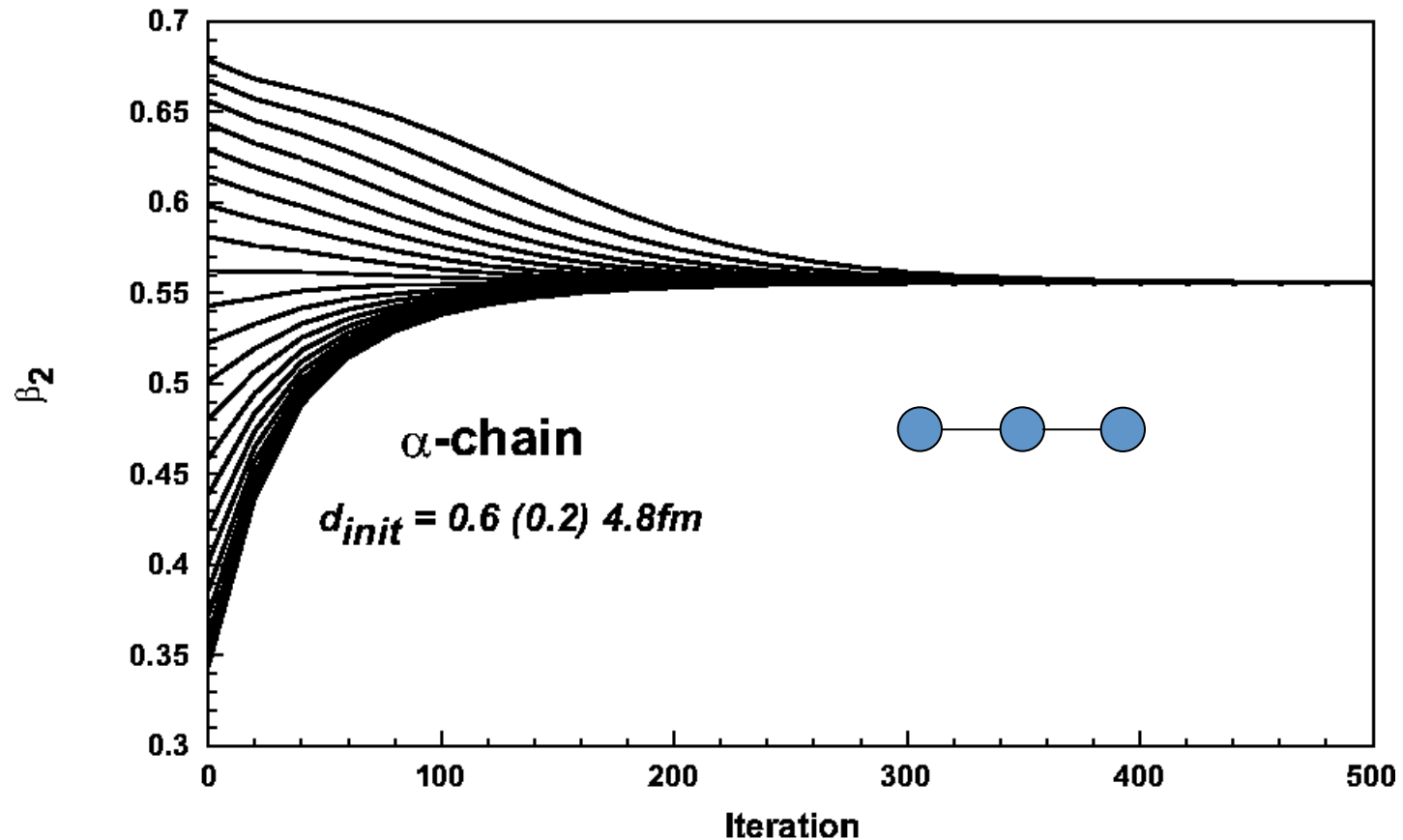
Force	E_{ls} [MeV]	β_2	Q_{20} [fm ²]	Cluster Analysis	
				\mathcal{O} [%]	σ
SkI3	13.5	-0.183	-90.3	28	1.92
SkI4	15.2	-0.171	-83.8	21	1.91
Sly6	15.1	-0.162	-81.0	17	1.93
SkM*	19.1	-0.133	-65.9	7	1.92
NL3		-0.186	-87.3	33	1.90
χ_m		-0.194	-94.1	29	1.89

³⁶Ar

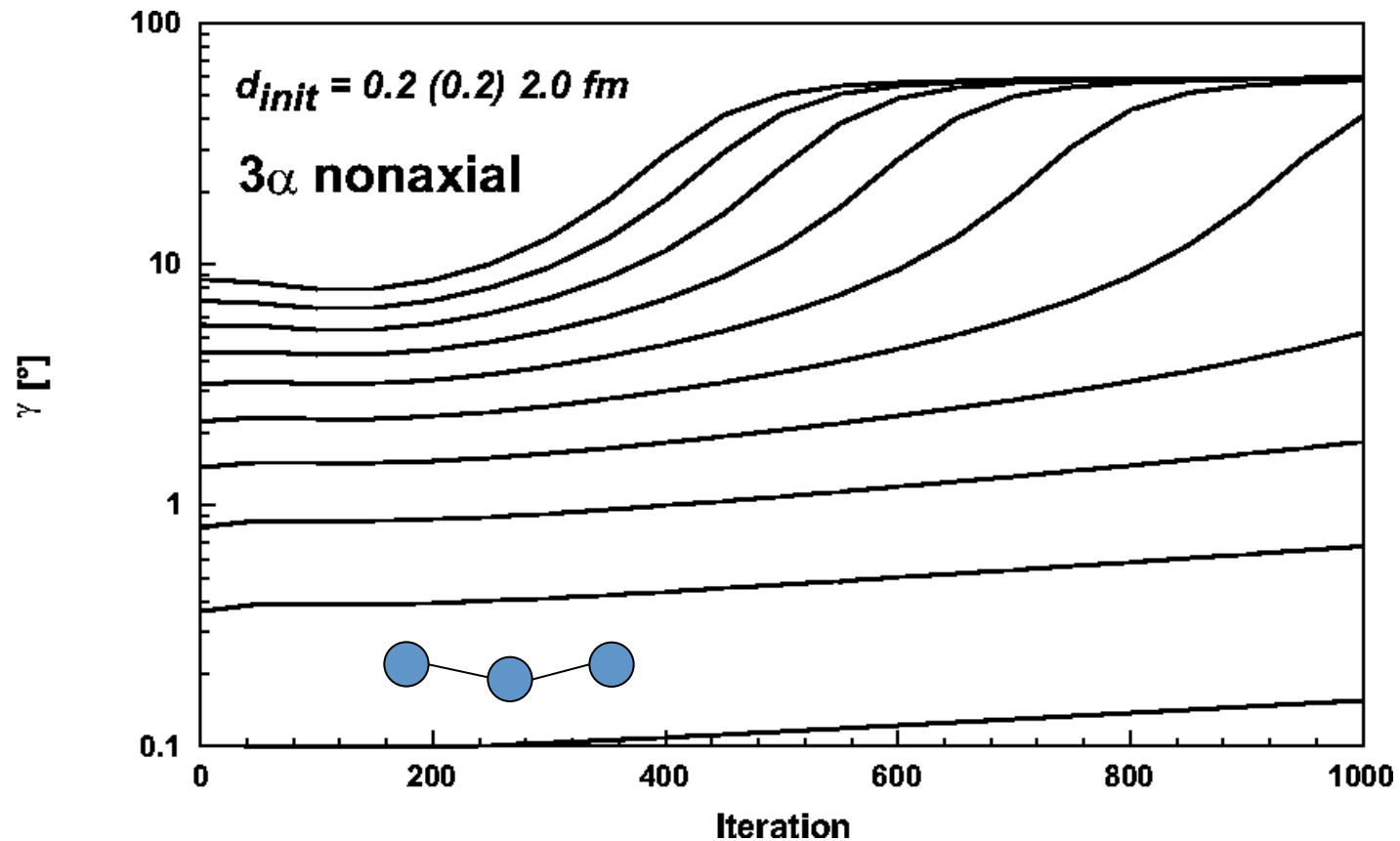
- α 's closely concentrated with random geometry
- overlap quite large: spin-orbit energy is reduced



Other Configurations: a 3- α Chain



Three- α -Chain Nonaxial

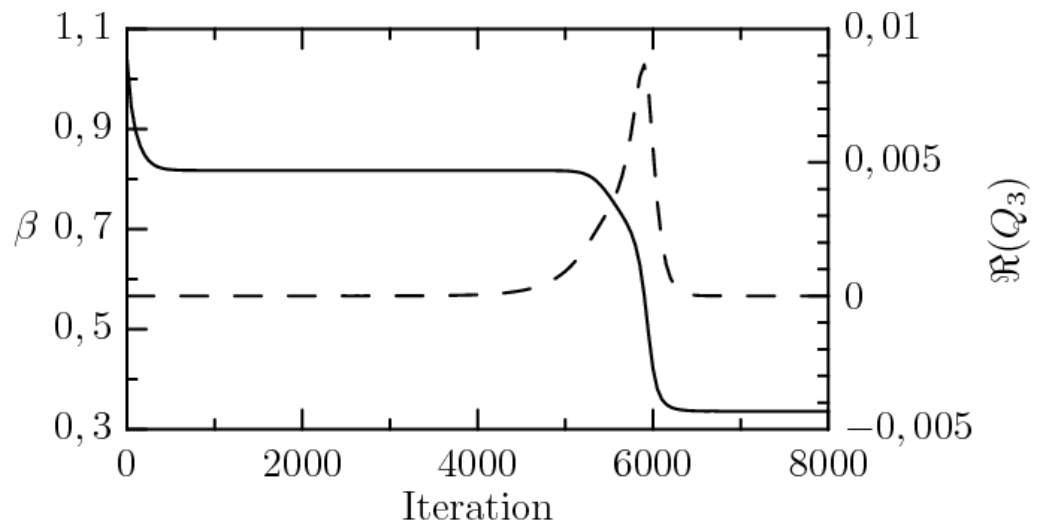
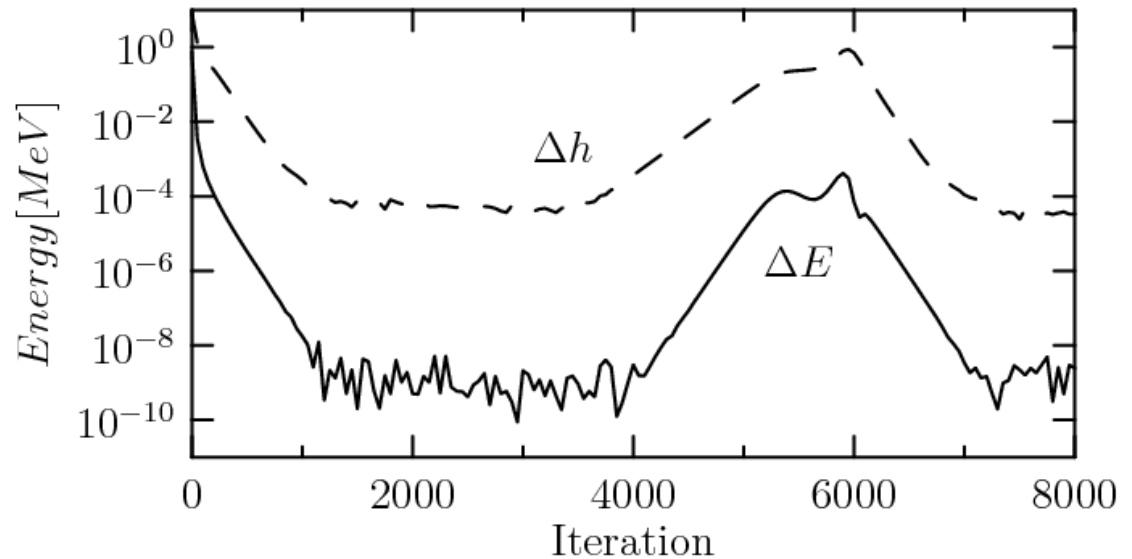


Convergence Behavior

An excited quasistable (?) state appears as an apparently converged configuration for 1000's of iterations. Sometimes convergence indicators are as good as for the ground state.

$$\Delta h = \frac{1}{A} \sum_{k=1}^A \sqrt{\langle \phi_k | \hat{h}^2 | \phi_k \rangle - \langle \phi_k | \hat{h} | \phi_k \rangle^2}$$

Subsequently, there is rapid conversion to the ground state via triaxial shapes.



Dynamic Stability

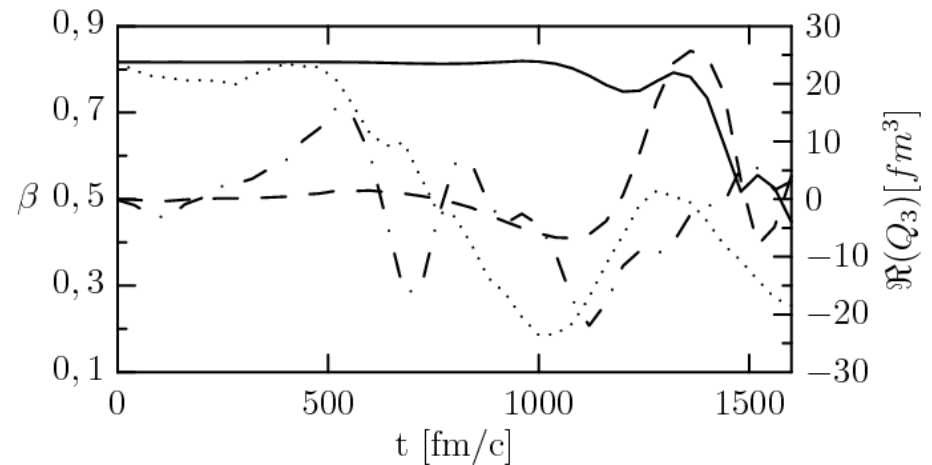
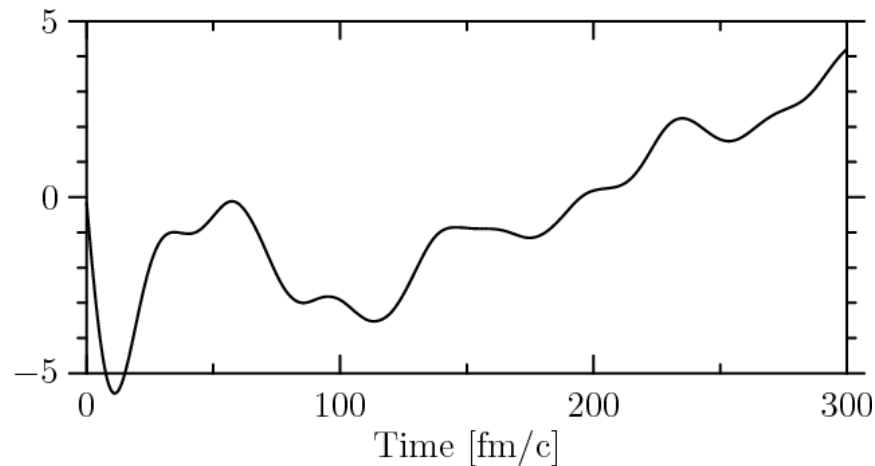
Give wave functions an initial boost factor
with $r=3\text{fm}$, $a=1\text{fm}$

$$A \frac{\exp e^{iQ(\vec{r})}}{1 + e^{(r-r_0)/\alpha}}$$

Then do time-dependent calculation.

Result shows long-term return to ground state, but some oscillations before.

Sample calculations for 0.04 and 2.83 MeV excitation energy



Rotational Stabilization of 4 α Chain

“Linear chain structure of four- α clusters in ^{16}O ”,

T. Ichikawa, J. A. Maruhn, N. Itagaki, and S. Ohkubo, PRL 107: 112501 (2011)

„Rod-shaped Nucleus“, Michelangelo d’Agostino, Phys. Rev. Focus, Sep. 9, 2011

Earlier results: H. Flocard, P. H. Heenen, S. J. Krieger and M. S. Weiss,
Prog. Theor. Phys. **72** (1984) 1000

- Static HF is done with a cranking constraint $-\omega j_y$
- Initialization is with four α -particles stretched in a non-axial configuration
- For fixed ω , the resulting total angular momentum J_y is calculated quantum mechanically and the moment of inertia and rotational energy factor determined as

$$\Theta = \frac{J_y}{\omega} \quad E_{rot} = \frac{\hbar^2}{2\Theta}$$

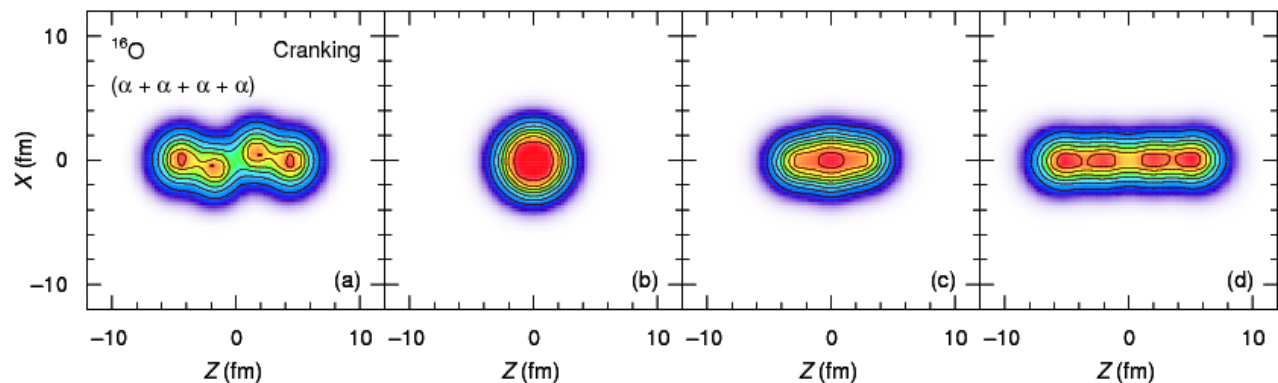
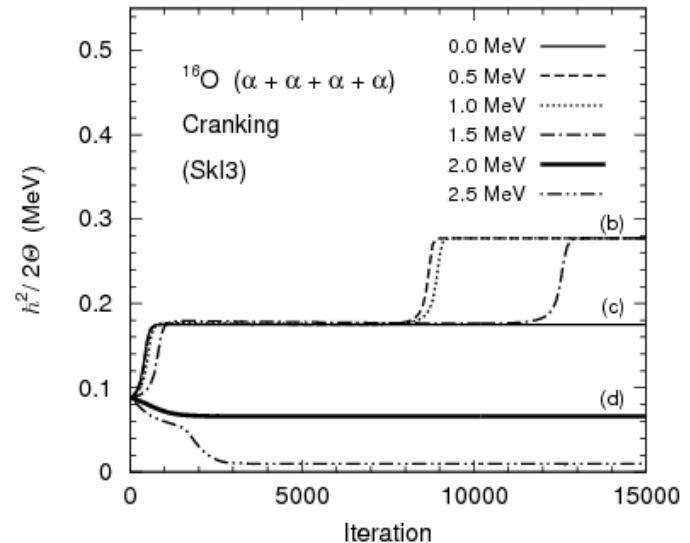
- Alternatively, the rigid-body moment can be calculated as

$$\Theta_{rigid} = \int (x^2 + z^2) \rho(\vec{r}) d^3r$$

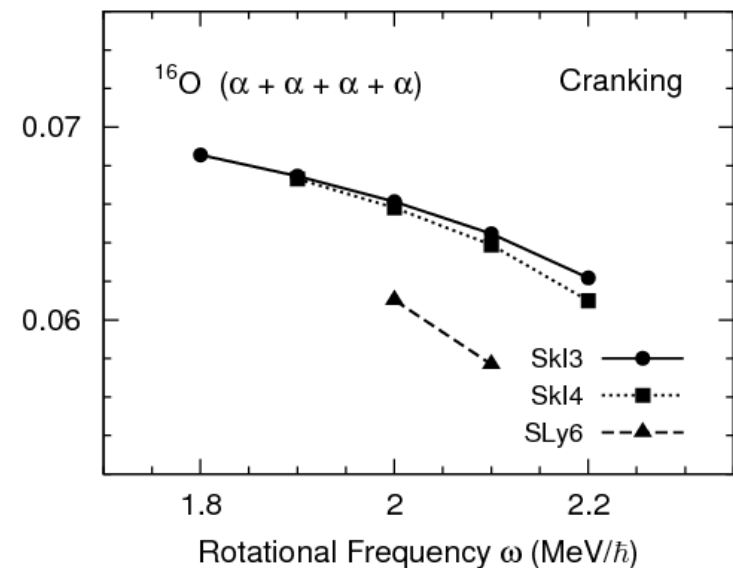
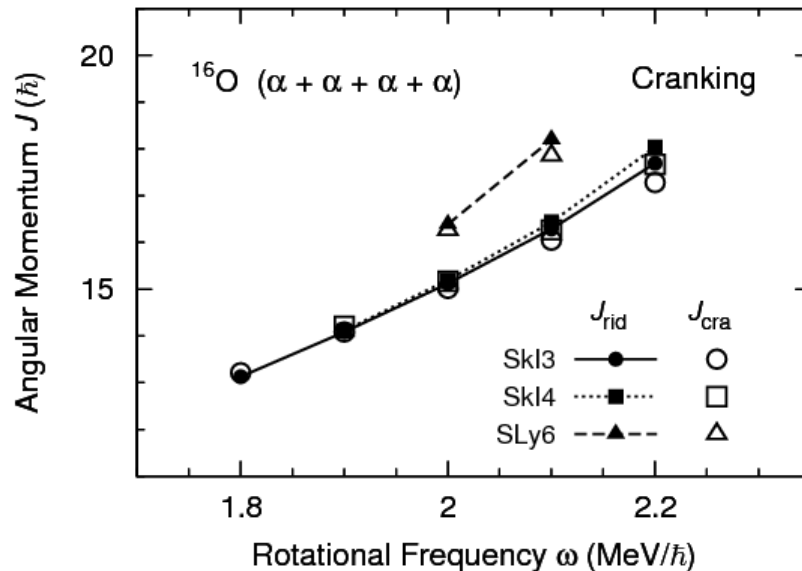
For the larger deformations both values agree quite well; for the spherical shape naturally ω and Θ vanish.

Resulting Convergence

- There is a range of angular momenta where the 4α chain is the convergence limit
- For smaller angular momenta, transition is to spherical via a deformed metastable state (note: for spherical rigid-body moment is given, quantal one is zero).
- For larger angular momenta, fission occurs



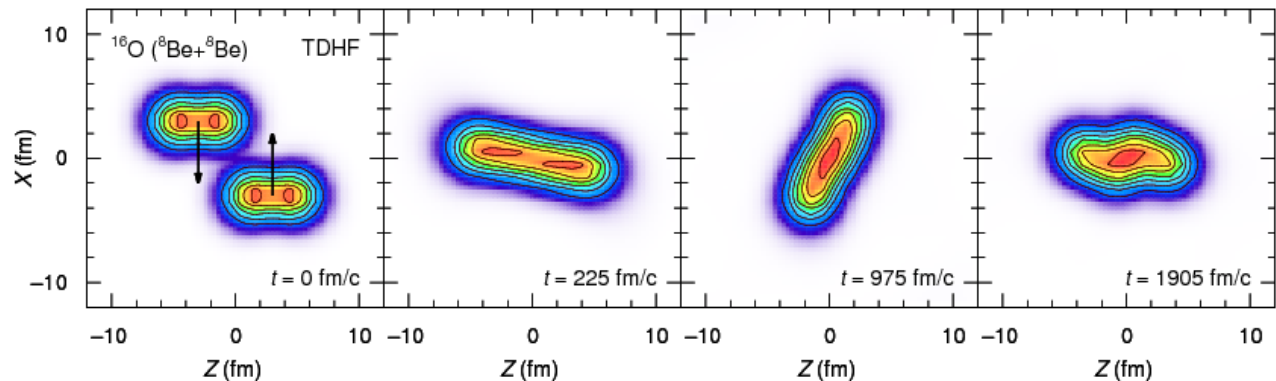
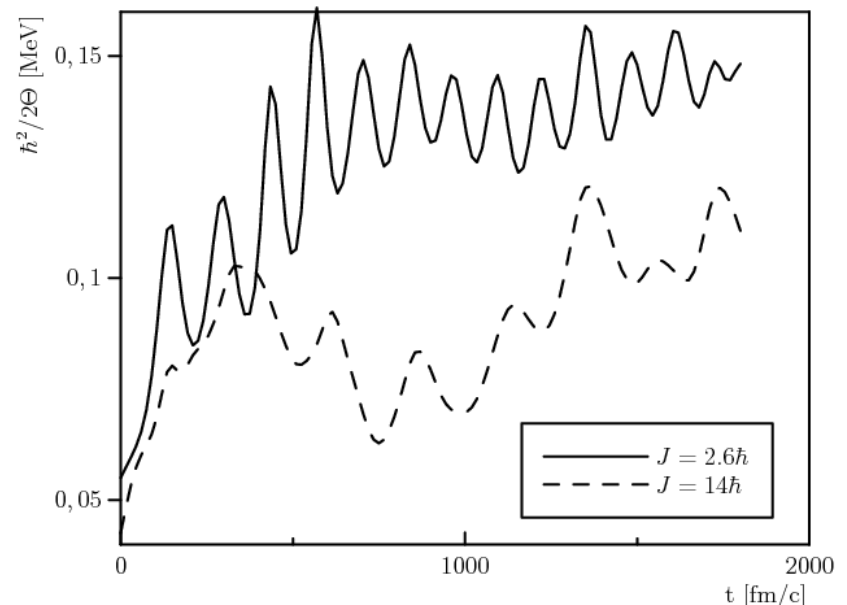
Range of Angular Momenta



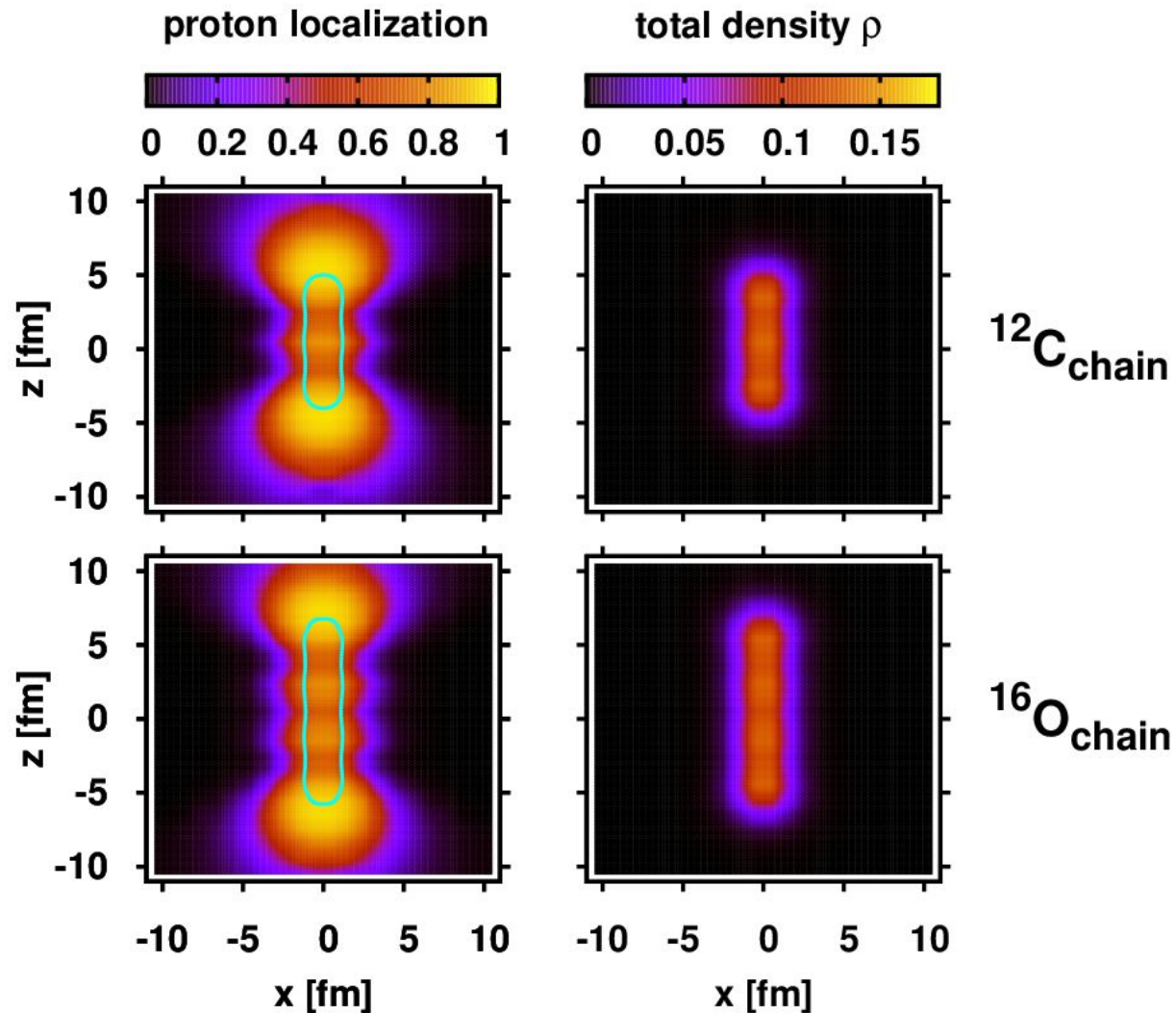
- The 4α chain is stabilized in a range of angular momenta around $13\text{--}18\hbar$. The quantal moment of inertia agrees quite well with the rigid-body value
- Axial symmetry is *restored* by rotation
- No stabilization was observed for 3α configurations

Role in Dynamics

- In a collision of ${}^8\text{Be}+{}^8\text{Be}$, a transient rotating chain state is visible but combined with strong oscillations
- Angular momentum helps to keep the rotating chain stabilized.
- This may play a role in astrophysical fusion situations



Localization for the Chain States



Ground State Binding Energies

	${}^4\text{He}$	${}^8\text{Be}$	${}^{12}\text{C}$	${}^{16}\text{O}$	${}^{20}\text{Ne}$
Exp.	28.3	56.5	92.2	127.6	160.6
SkI3	27.8	49.7	89.3	128.9	156.8
SkI4	27.7	49.8	89.3	128.6	157.3
SLy6	27.2	49.0	88.6	127.4	155.9
SkM*	26.8	50.1	93.5	128.0	157.9
NL3	33.9	52.9	91.2	128.7	156.6
χ_m	39.3	53.6	88.9	132.3	161.9
	${}^{24}\text{Mg}$	${}^{28}\text{Si}$	${}^{32}\text{S}$	${}^{36}\text{Ar}$	
Exp.	198.3	236.5	271.8	306.7	
SkI3	194.7	233.0	267.1	304.8	
SkI4	196.11	234.9	269.4	305.5	
SLy6	194.4	233.1	268.5	304.0	
SkM*	197.6	237.9	275.1	305.5	
NL3	194.1	231.8	265.6	302.2	
χ_m	197.0	235.0	269.5	308.8	

Initialization for ^{16}C

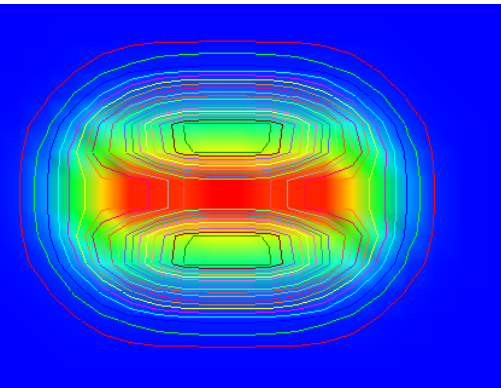
- For three α -clusters Gaussians at $z=0, -d$, and $+d$, with d usually 3 fm. Width 1.8 fm.
- σ -state neutrons added as distorted Gaussians (3 times larger width in z -direction) multiplied by $z(z-d)$
- π -state neutrons similar with factor $(x+isy)$. s for spin direction, r for regular ($r=1$) π' and irregular ($r=-1$) π .
- δ -states use factor $(x+isy)z$.
- In the results, π' have $j_z=\pm 1/2$, π have $j_z=\pm 3/2$
- Both for time-reversal invariant and other states, HF-3D produces the angular-momentum quantization very well.

Initial		Final
Name	Spins	States
$\pi^2\sigma^2$	+ - + -	$\pi^2\pi'^2$
$\pi^2\sigma\pi$	+ - + -	$\pi^2\sigma\pi'$
$\pi^2\sigma\pi'$	+ - + +	$\pi^2\pi'^2$
$\pi^2\delta^2$	+ - + -	$\pi^2\delta^2$
$\pi^2\delta\pi$	+ - + -	$\pi^2\delta\pi'$
$\pi^2\delta\pi'$	+ - + +	$\pi^2\delta\pi''$

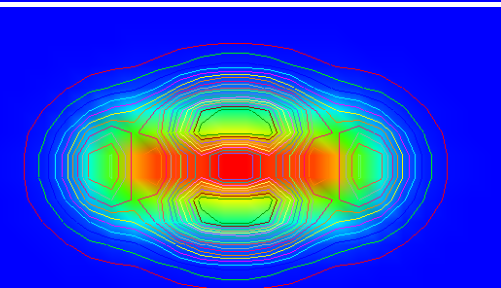
Observed states: contain 2/3 probability for 3-a chain

Force	E_B	$\pi^2 \delta^2$	$\pi^2 \pi'^2$	$\pi^2 \delta \pi'$	$\pi^2 \sigma \pi'$	$\pi^2 \delta \pi''$
SkI3	101.5	19.5	14.5	17.0	19.1	17.5
SkI4	100.8	19.9	15.7*	17.6	19.7	18.0
Sly6	100.6	18.9	15.4*	17.0	19.0	17.3
SkM*	115.0	17.5	16.4*	16.9	19.7	17.0

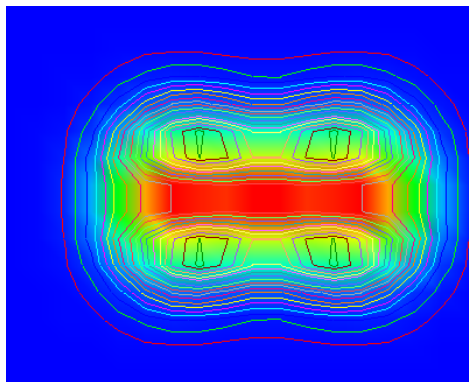
Force	$\beta_{g.s.}$	$\pi^2 \delta^2$	$\pi^2 \pi'^2$	$\pi^2 \delta \pi'$	$\pi^2 \sigma \pi'$	$\pi^2 \delta \pi''$
SkI3	0.34	0.82	0.69	0.76	0.88	0.76
SkI4	0.33	0.80	0.68*	0.75	0.86	0.74
Sly6	0.32	0.81	0.68*	0.75	0.87	0.75
SkM*	0.28	0.79	0.66*	0.73	0.85	0.73



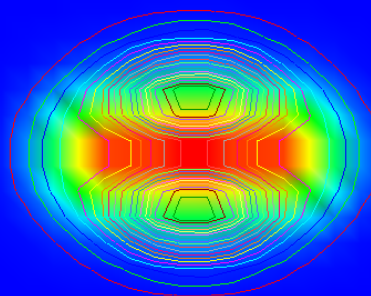
$K^p=1^-$



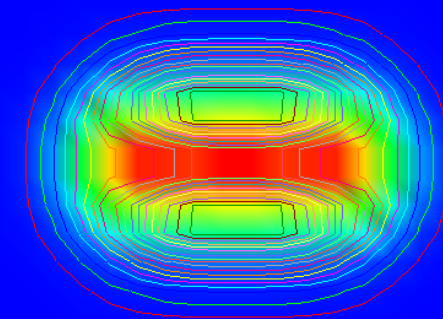
$K^p=1^+$



$K^p=0^+$



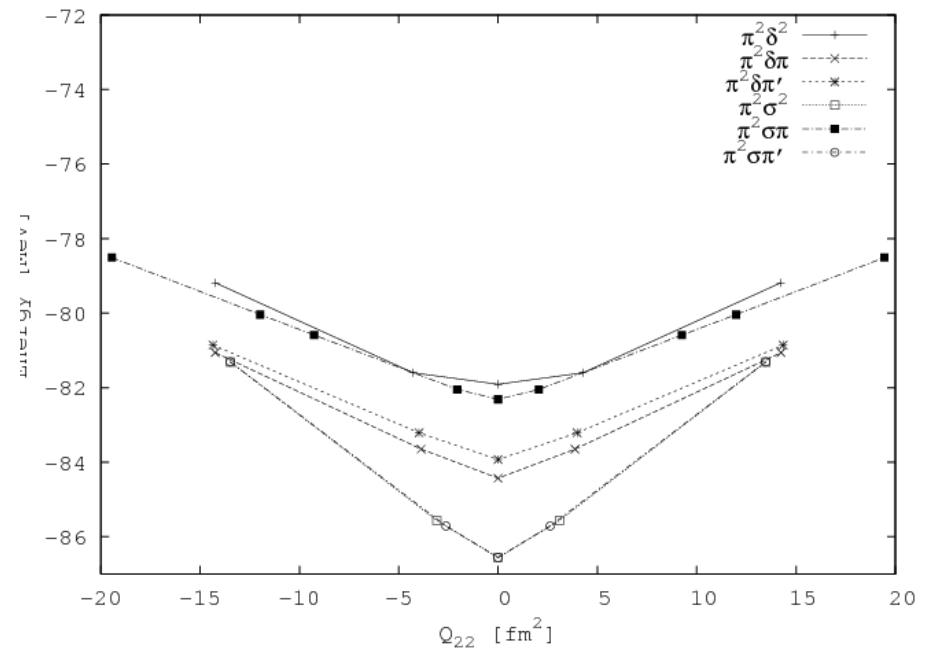
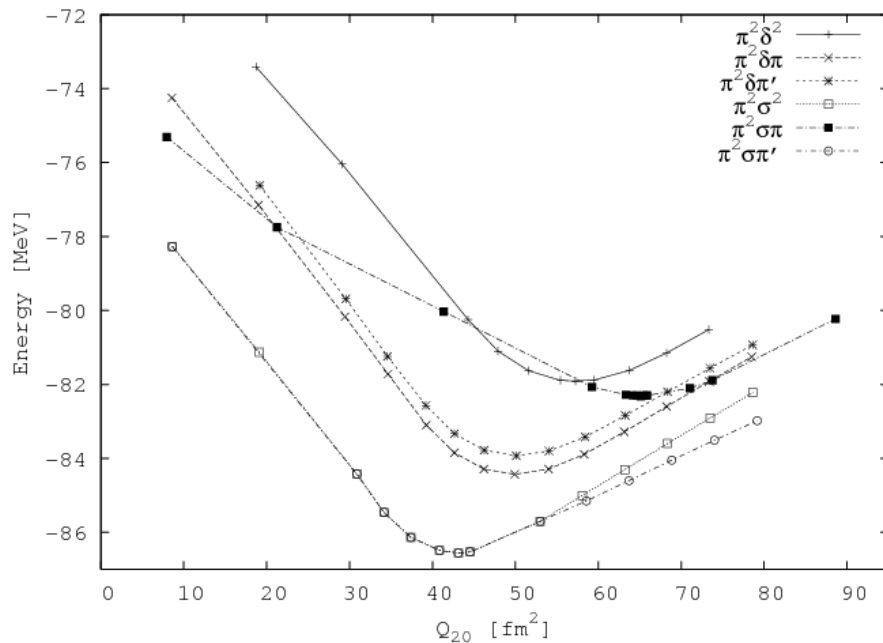
$K^p=0^+$



$K^p=2^+$

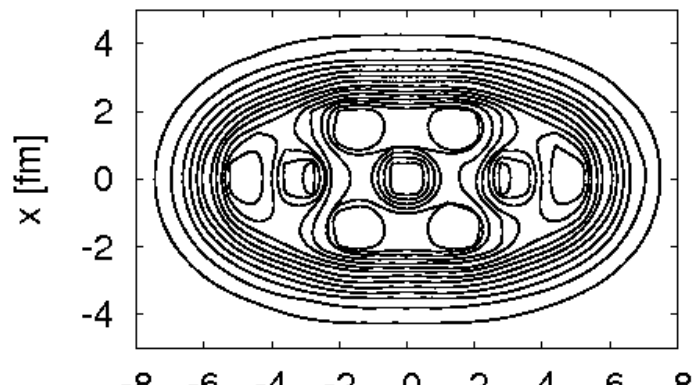
Stability: Static Quadrupole

- Check stability using quadrupole constraint
- (N. Löbl)

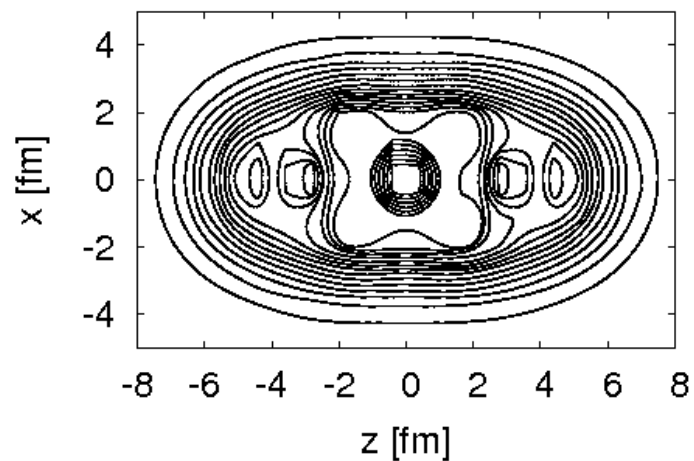
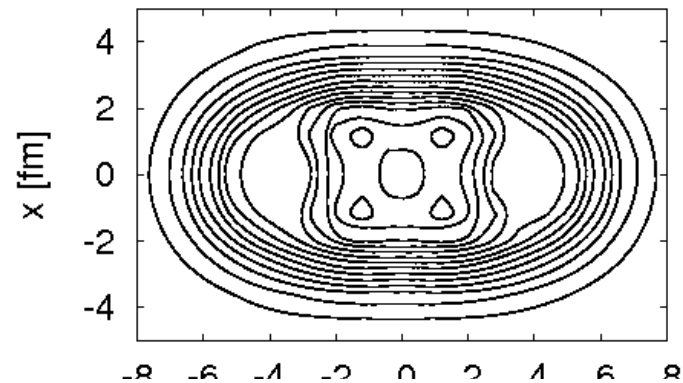


^{20}C Chain States

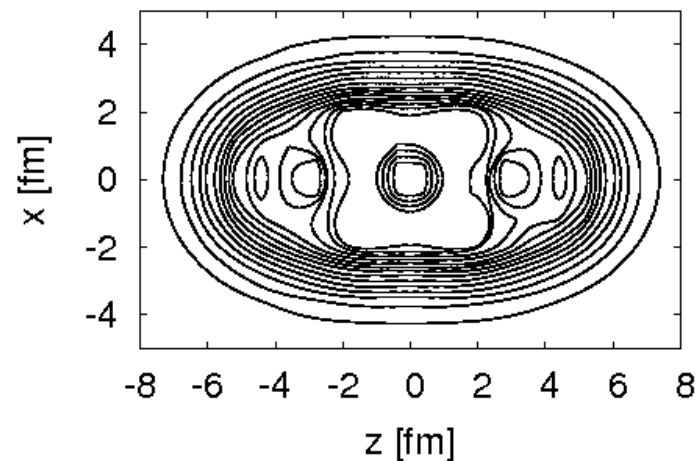
SkI3



SkI4



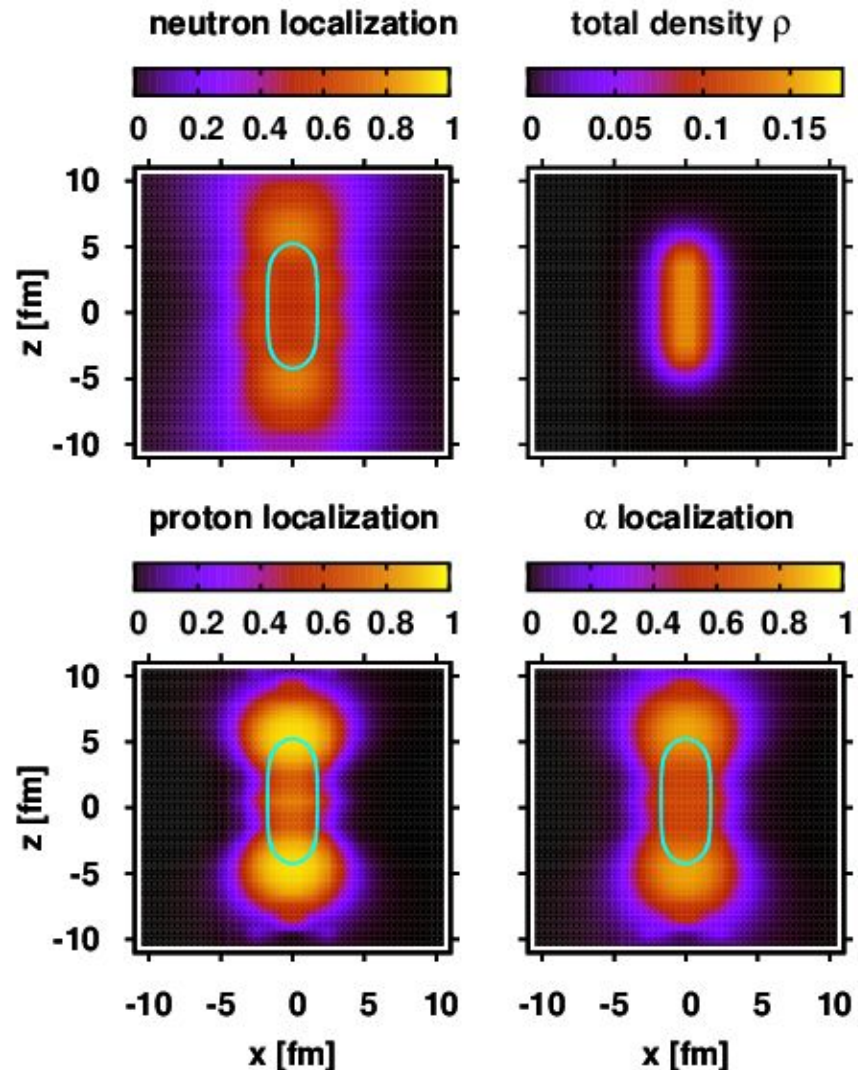
Sly6



SkM*

Localization for ^{20}C

- Localization is quite different for p and n
- Protons show higher degree of localization
- Average still shows some remnants



Properties and Dynamic Stability

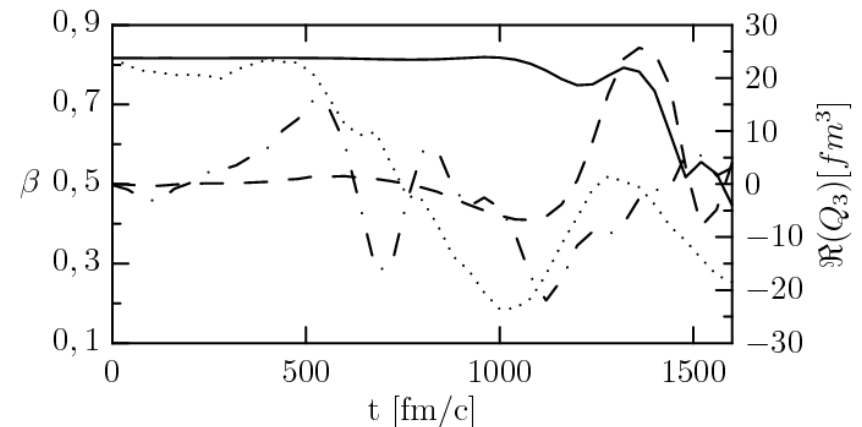
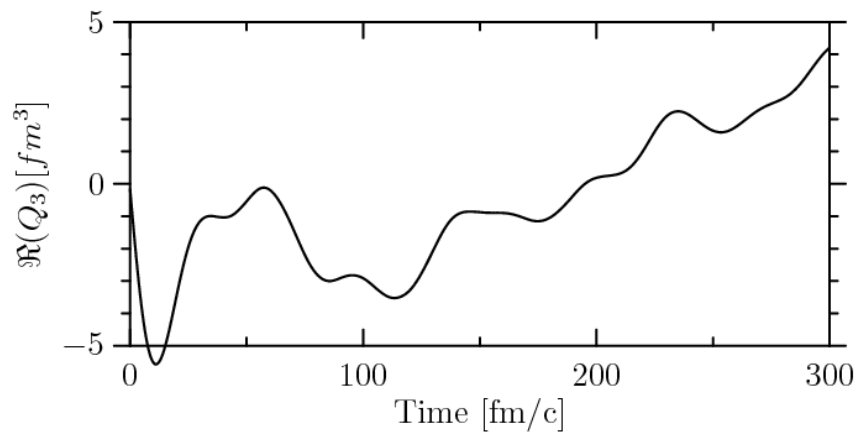
Force	Dh $\times 10^6$	n	E_B (g.s.)	E^*	b_2
SkI3	21	>50000	113.37	14.48	0.851
SkI4	14	12000	108.11	14.71	0.824
Sly6	22	19000	109.73	14.95	0.837
SkM*	23	9000	128.67	17.06	0.823

Give wave functions an initial boost factor with $r=3\text{fm}$, $a=1\text{fm}$

Then do time-dependent calculation.

Result shows long-term return to ground state, but some oscillations before.

Sample calculations for 0.04 and 2.83 MeV excitation energy

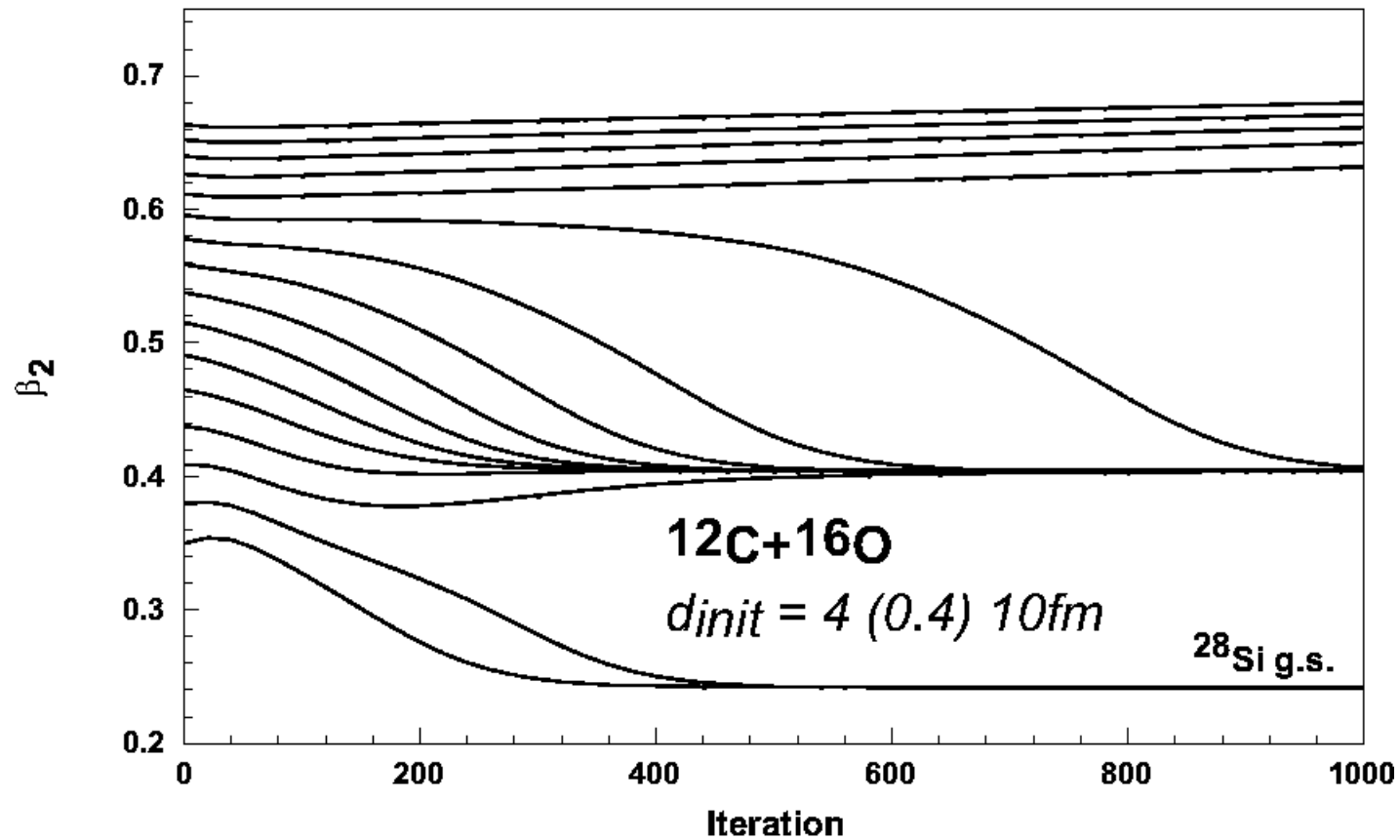


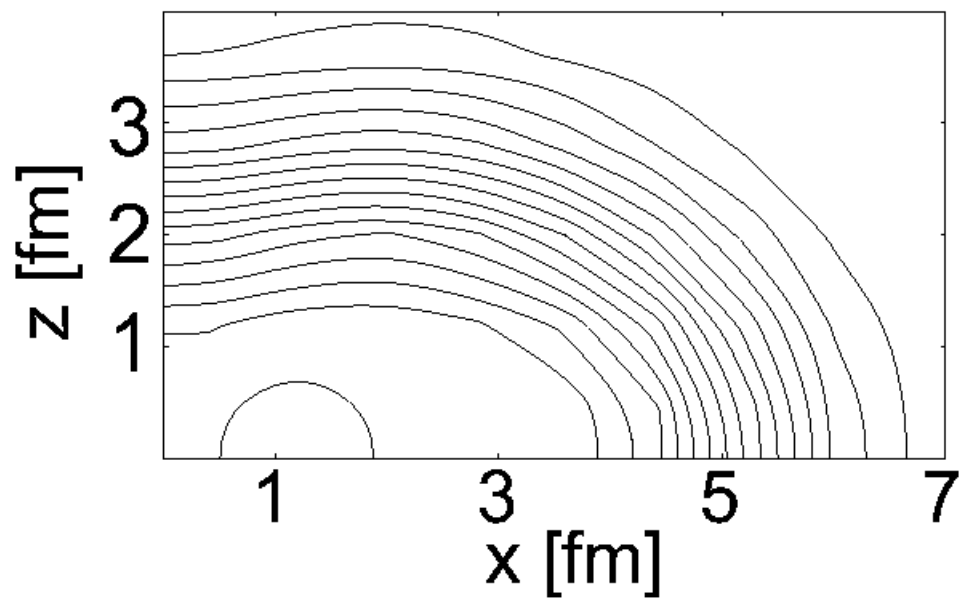
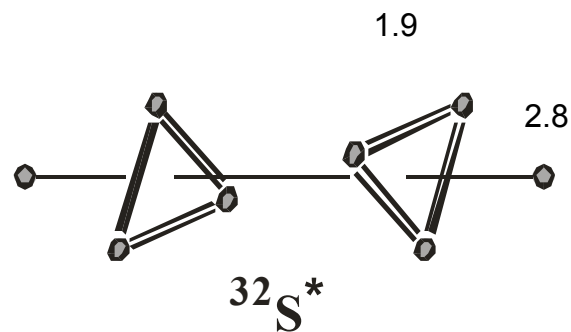
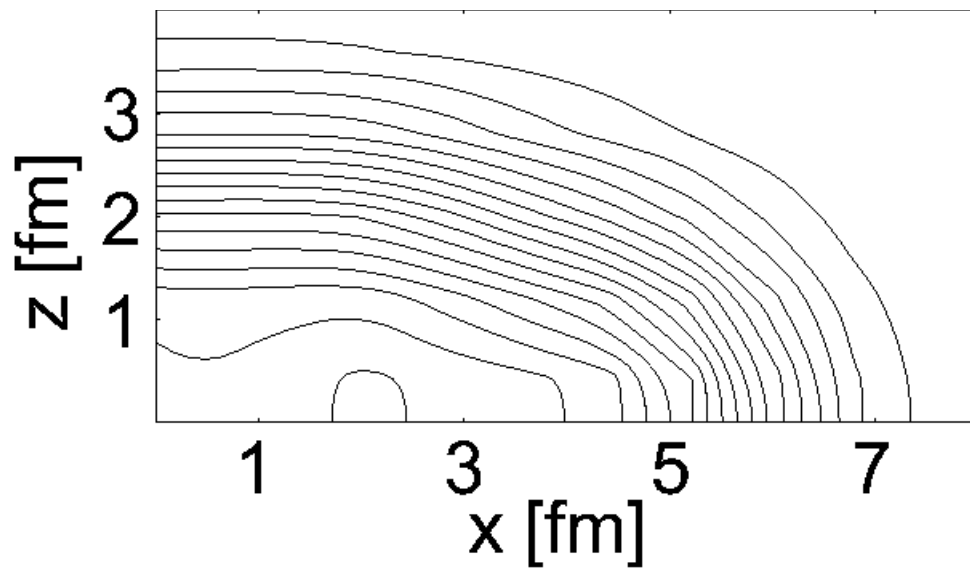
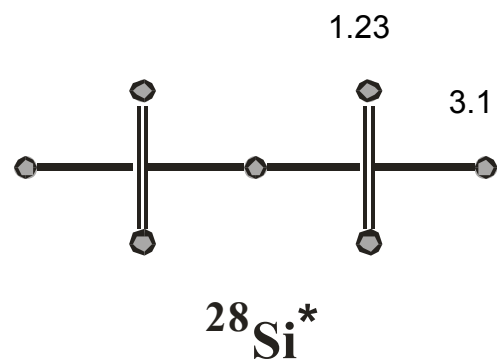
Superdeformed States

- Calculated by initializing with fragment ground states at a distance
- In practice converge to symmetric configuration (i.e. $^{12}\text{C}+^{20}\text{Ne}$ identical to $^{16}\text{O}+^{16}\text{O}$)
- Pairing is important

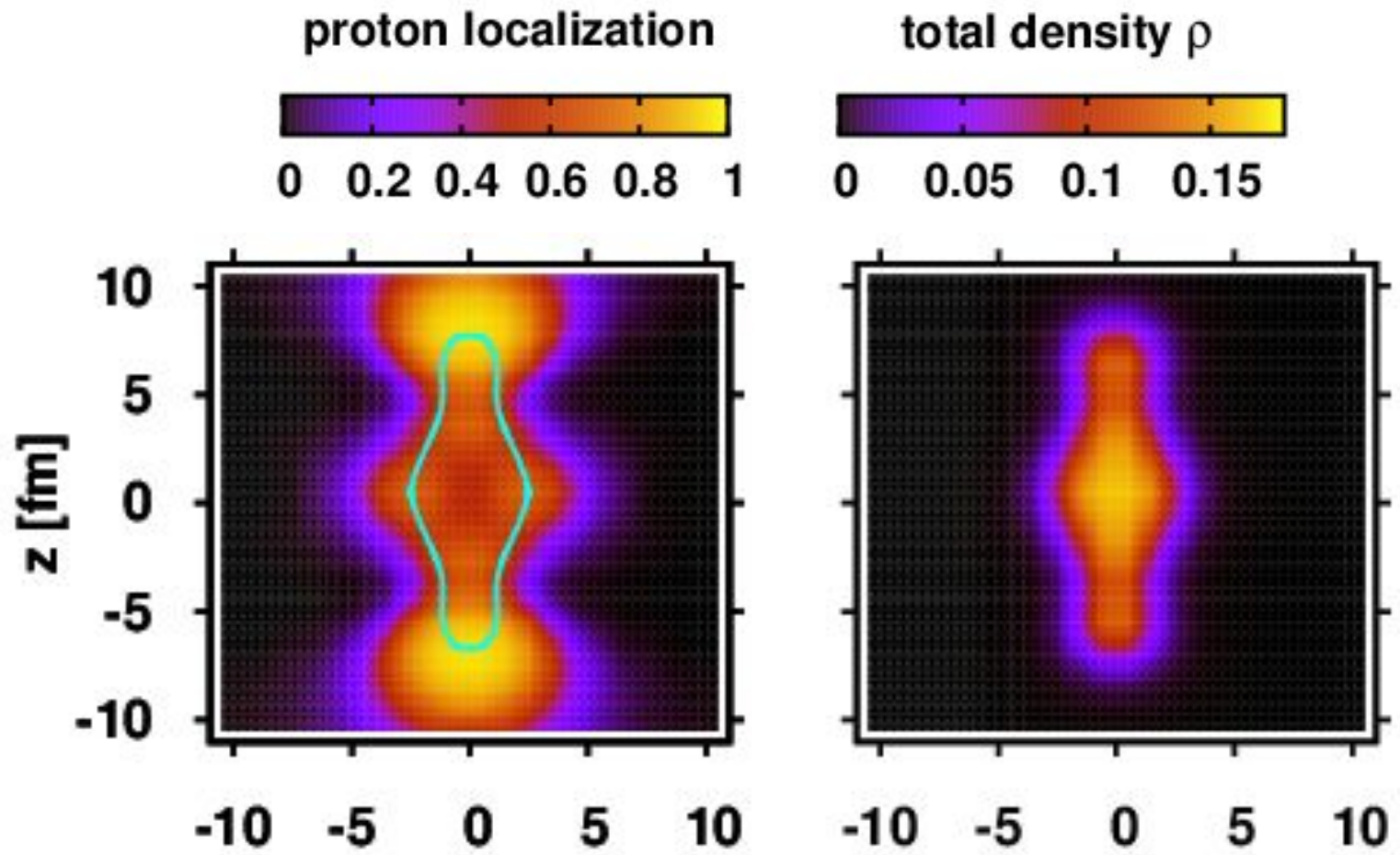
System	E^* [MeV]	E_{ls} [MeV]	β_2	Q_2 [fm ²]	Cluster Analysis	
					\mathcal{O} [%]	σ [fm]
SKI3						
^{28}Si	13.2	25.6	0.773	325.9	1.3	1.80
^{32}S	8.9	12.3	0.737	377.4	34.5	1.79
^{36}Ar	8.7	29.1	0.529	283.4	3	1.88
^{40}Ca	26.3	28.1	0.983	859.8	0.8	1.80
χ_m						
^{28}Si	11.1		0.775	314.4	1.2	1.77
^{32}S	5.7		0.743	368.6	36.2	1.75
^{36}Ar	9.2		0.533	278.9	1.2	1.84
^{40}Ca	23.7		0.982	829.41	0.8	1.77

Convergence

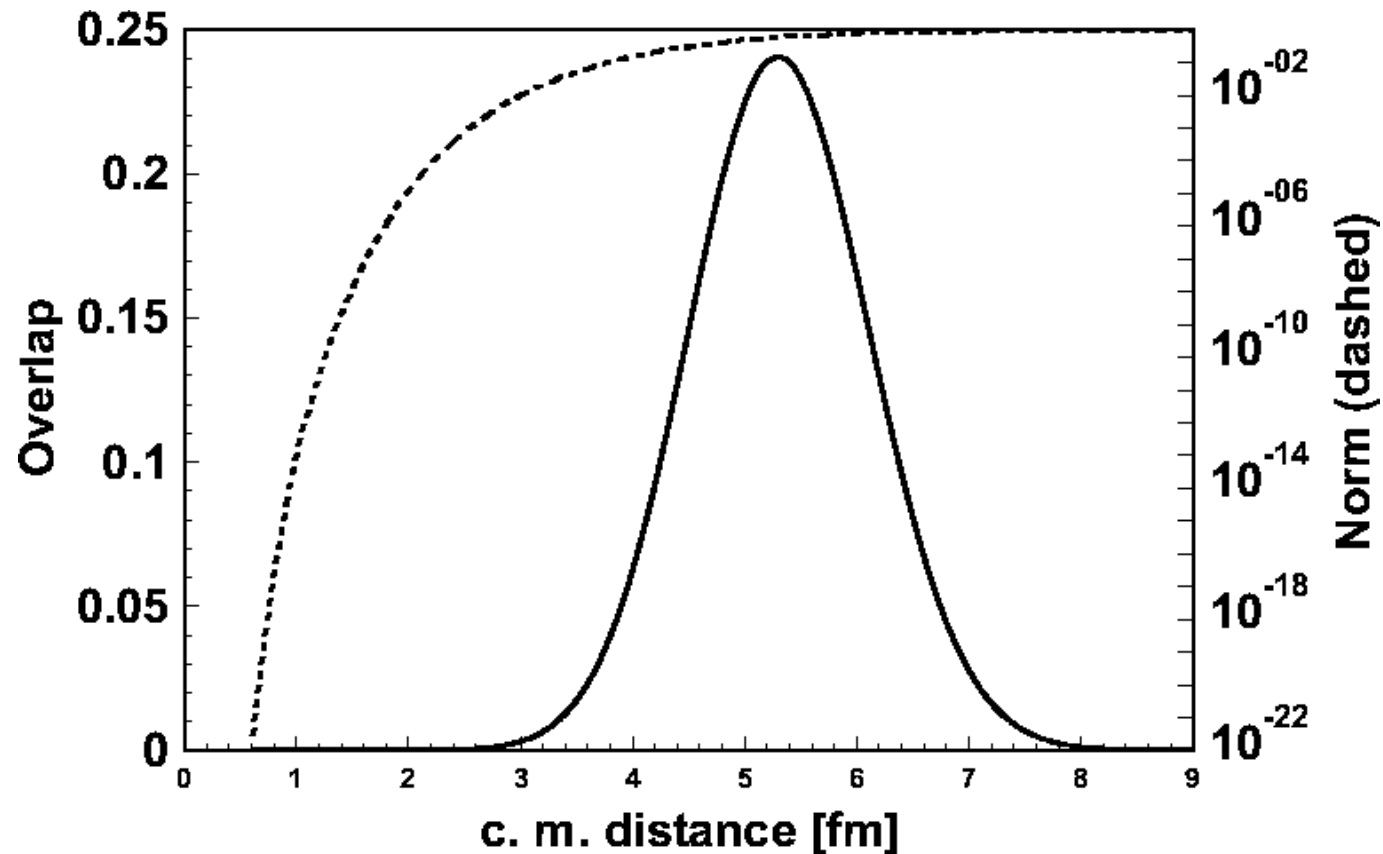




Localization in ^{28}Si Isomer

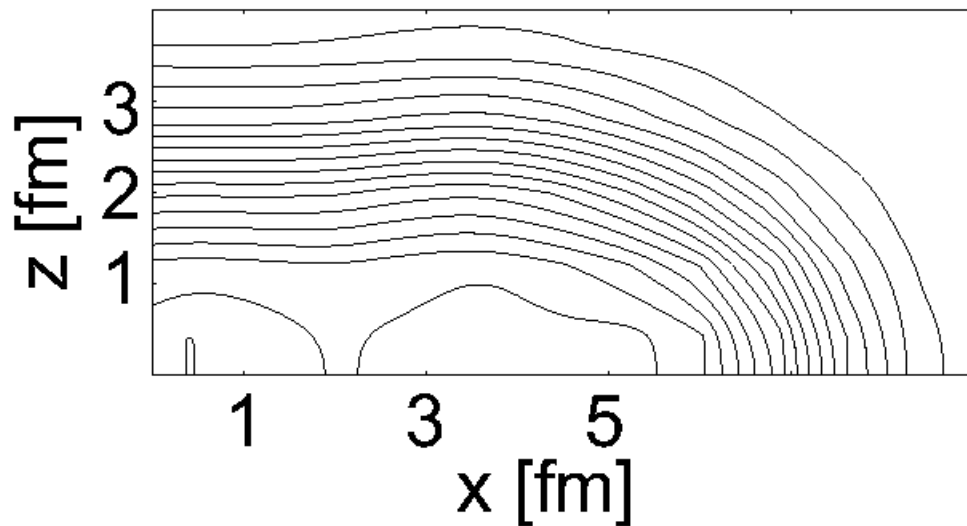
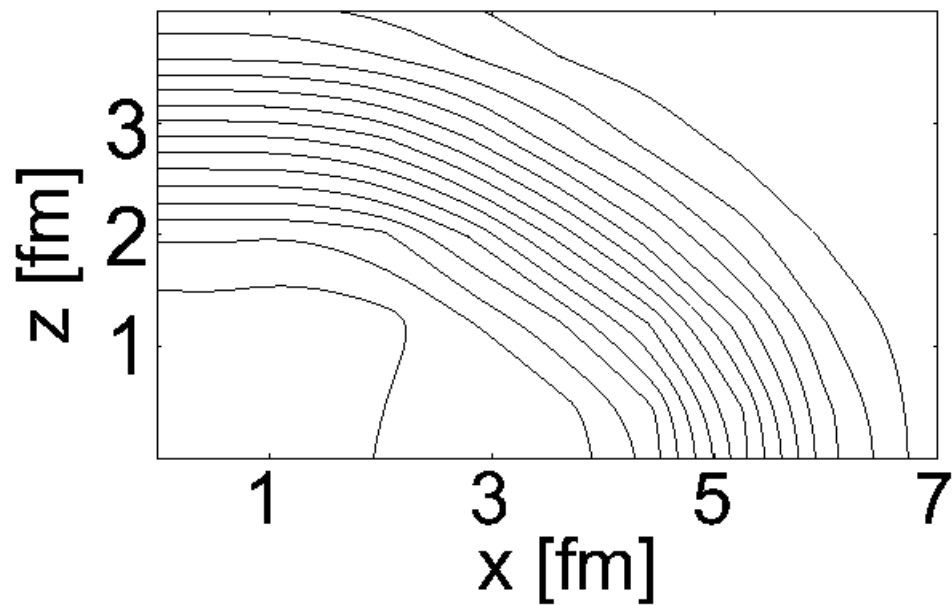
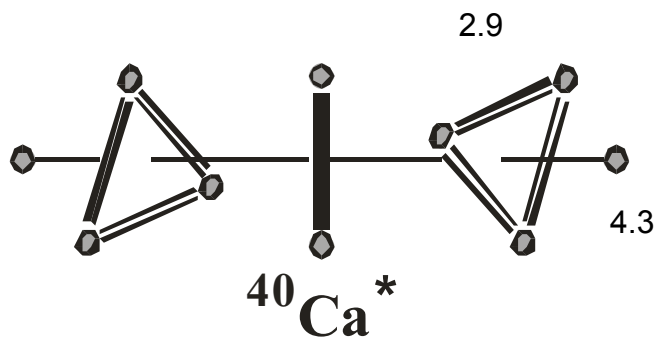


- Interpretation of ^{32}S superdeformed state as $^{16}\text{O}+^{16}\text{O}$ molecular configuration

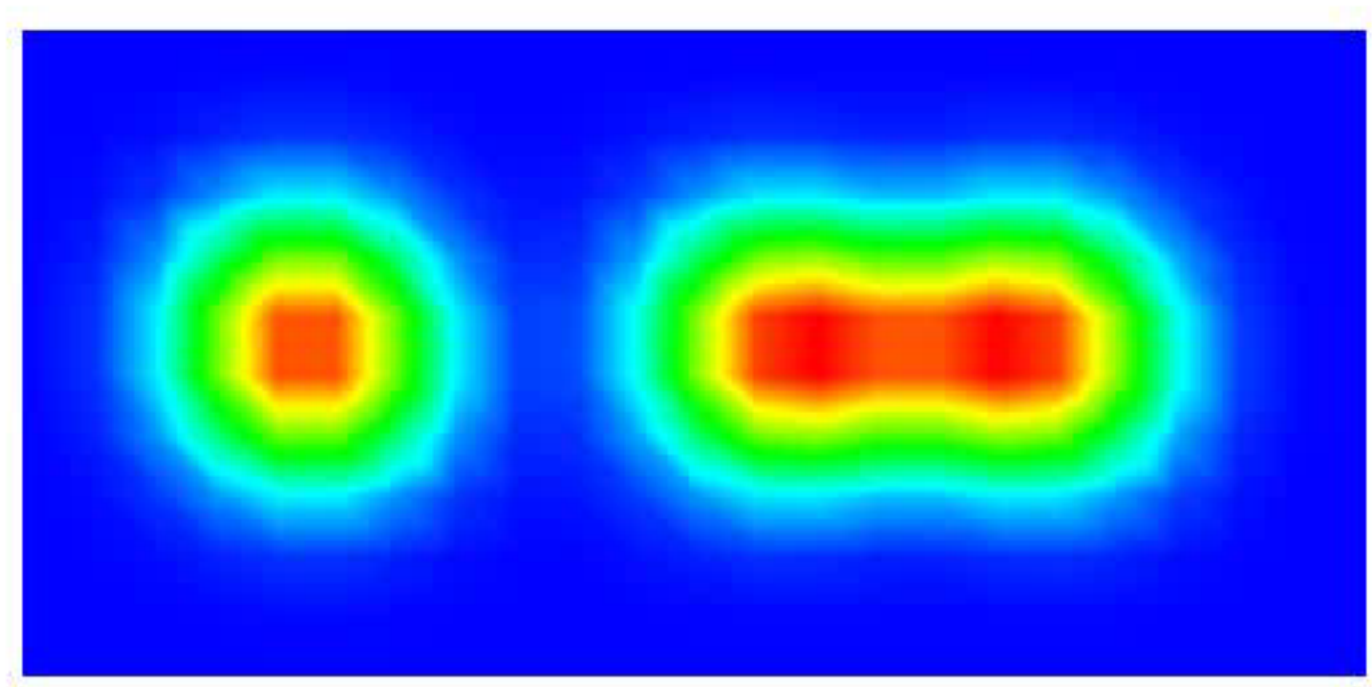


^{36}Ar

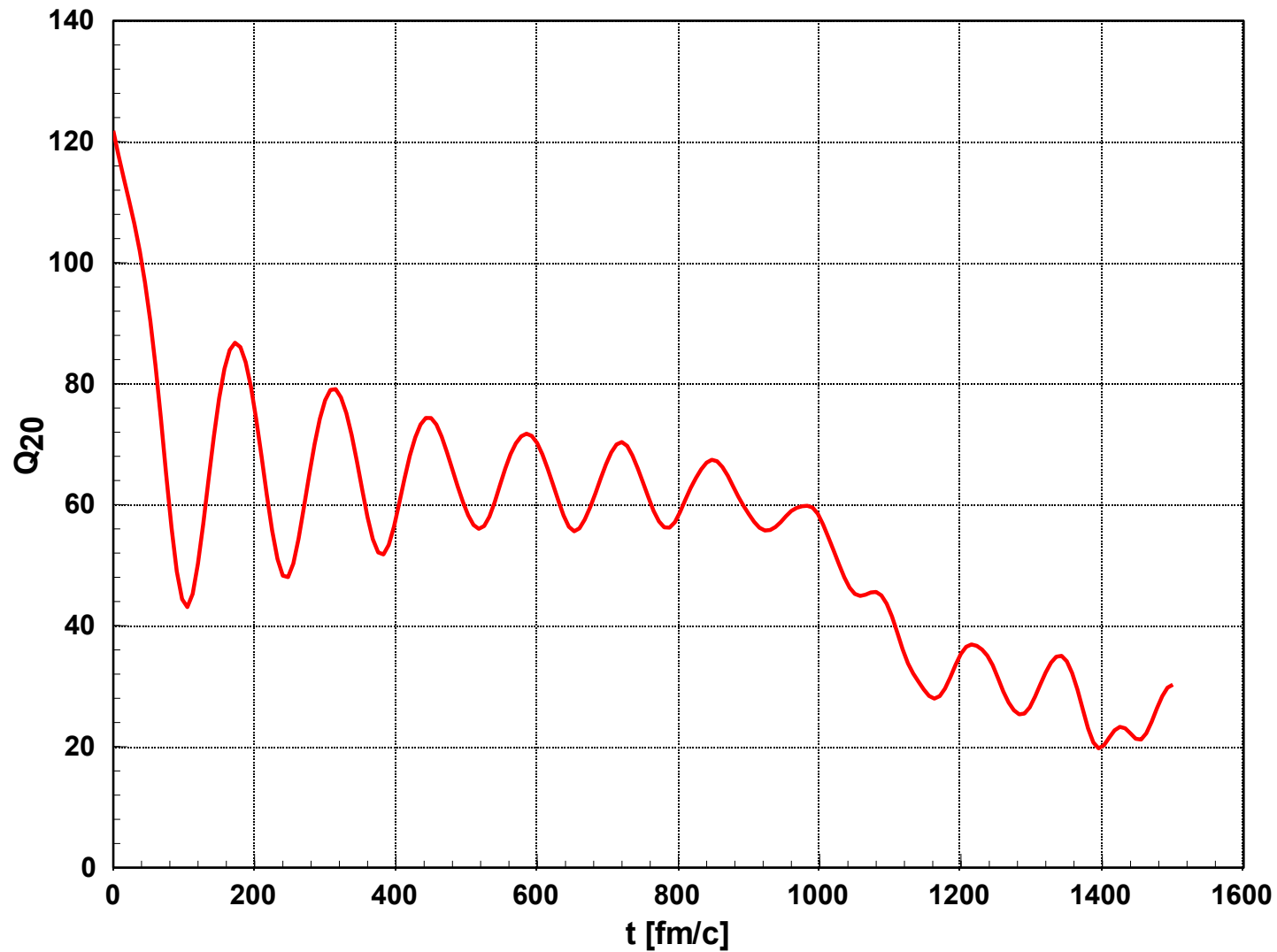
a configuration
not well
determined



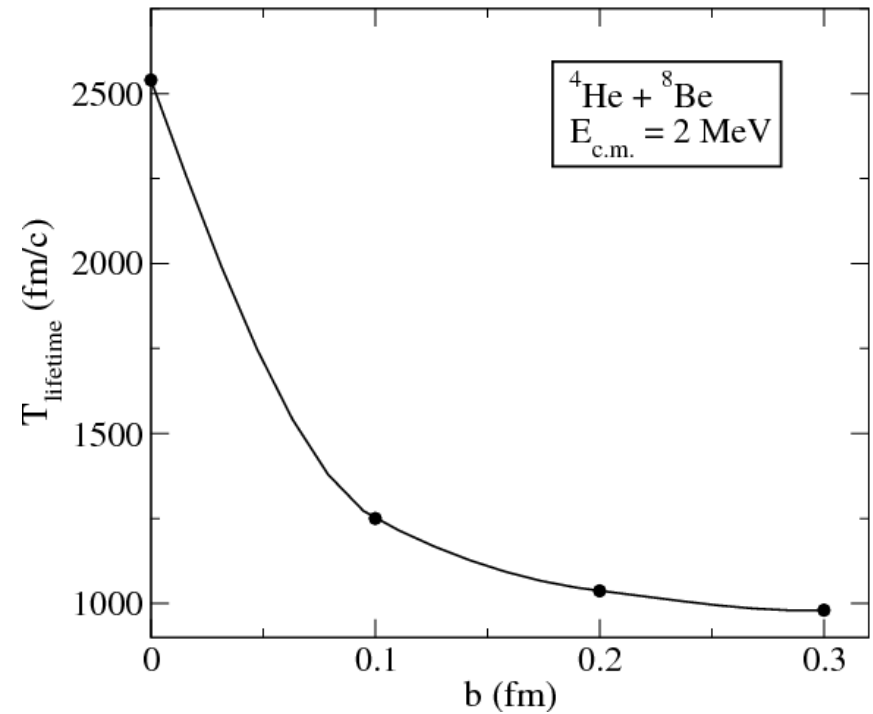
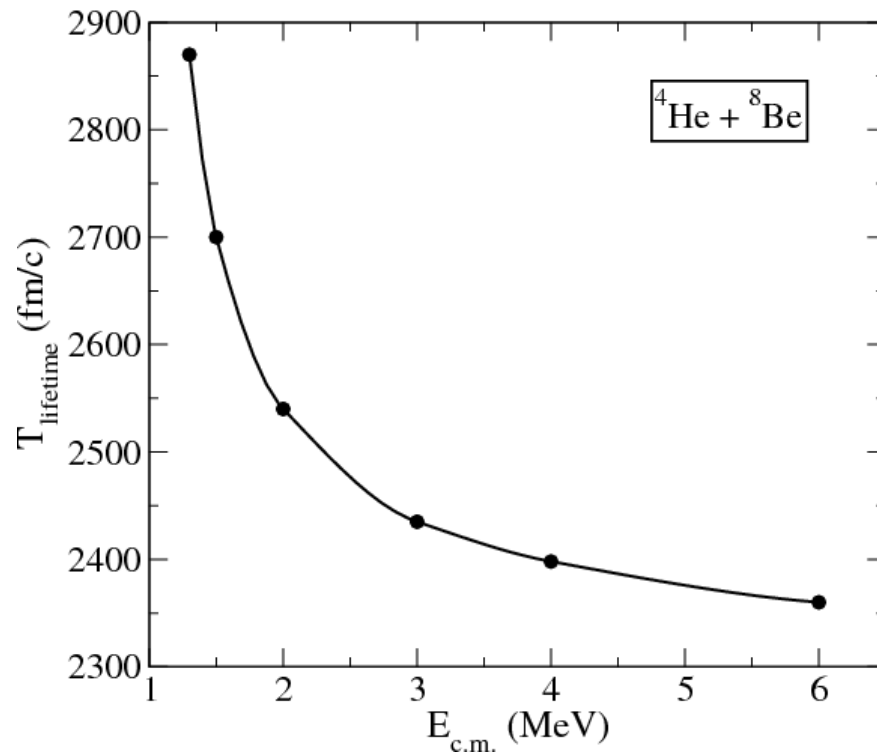
$4\text{He} + 8\text{Be}$ at $b=0.2\text{ fm}$



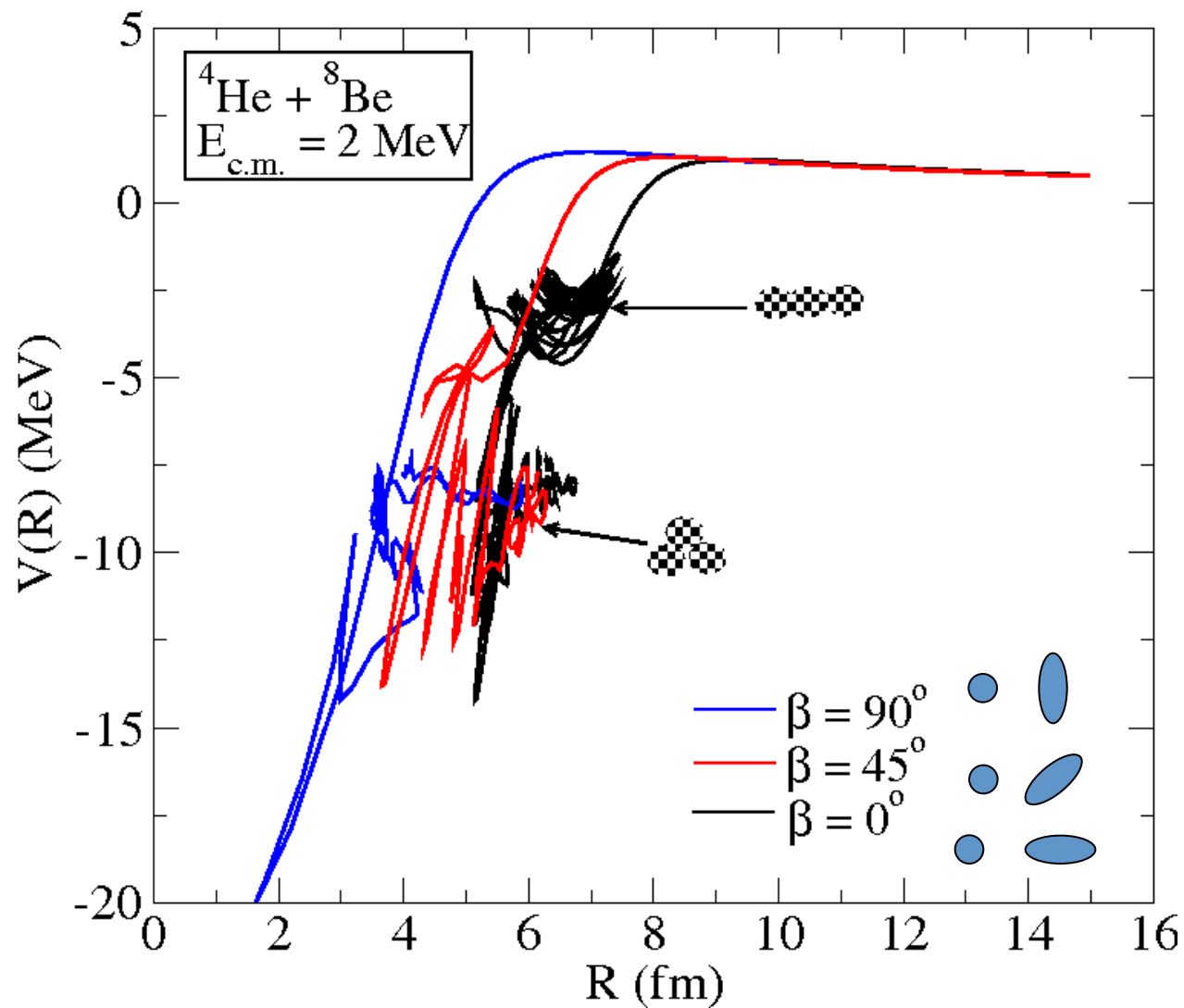
$Q_{20}(t)$ for $b=0.2\text{fm}$



Dependence on b and $E_{\text{c.m.}}$

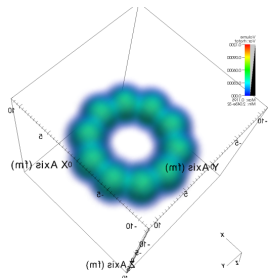


Successive Mode Coupling



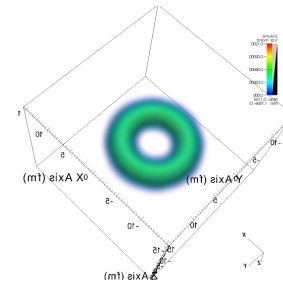
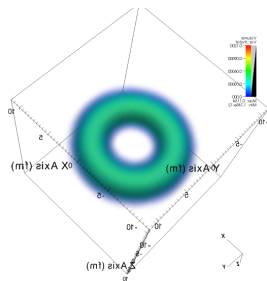
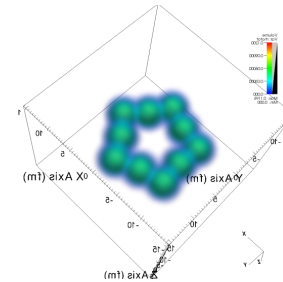
Toroidal Nuclei

- Originally proposed by C. Y. Wong Phys. Lett. B41, 446 (1972)
- Also studied stability against rotation and “sausage” deformations in a liquid-drop approach
- Recently also looked at very heavy systems in a Skyrme-force Hartree-Fock approach



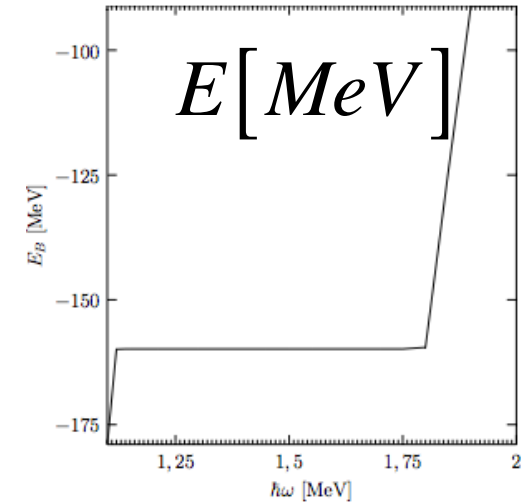
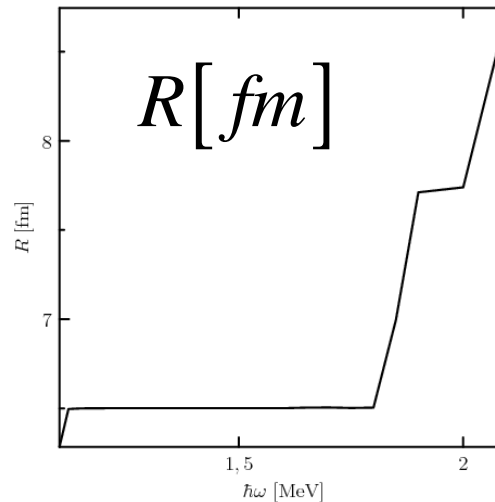
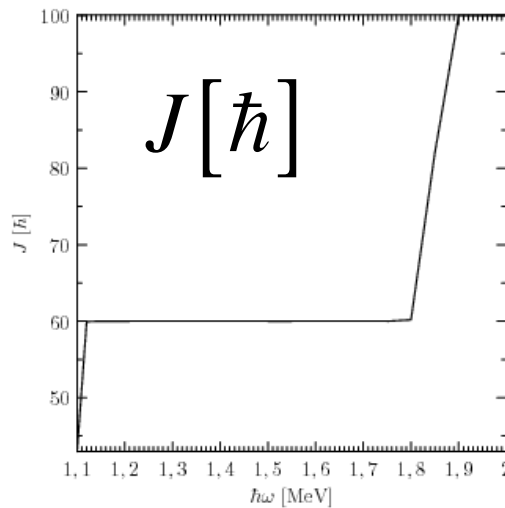
The 10- α Ring

- Static HF with cranking constraint around symmetry axis
- No clustering seen
- Starting with an initial distorted configuration also leads to a smooth ring.



Properties of the States

- Very precisely quantized J , but different values can occur
- R.m.s. radius varies with J



Excitation energy 176 MeV

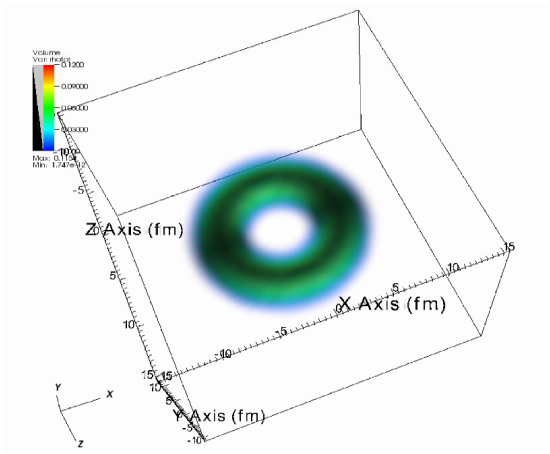
- Concrete results for Sly6

Quantization of J

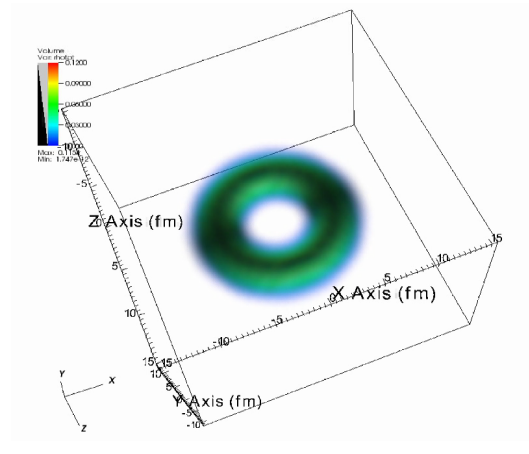
- The s.p. states are of the type $\eta(\rho)\chi(z)\exp(im\phi)$ with the z and r directions in the ground state
- Isospin and spin are approximately degenerate, with 4 particles per s.p. state
- The total angular momentum is generated by having an asymmetric occupation of m-states (K-isomers)
- The occupation of m-states is
 - Either from -3...+6: resulting $J=4*(4+5+6)=60$
 - Or from -2...+7: resulting $J=4*(3+4+5+6+7)=100$These are the values seen in the numerical results.

Cutting up the Ring

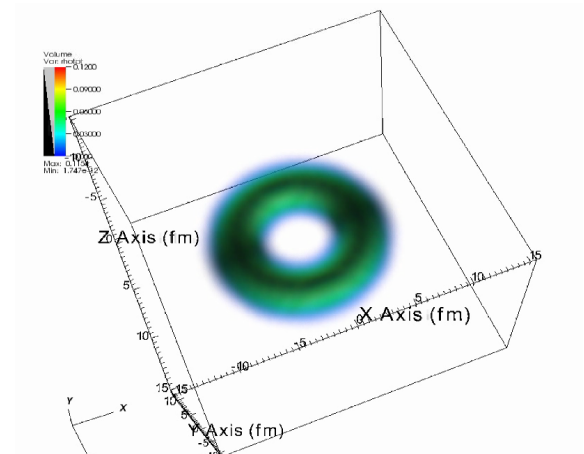
A time-dependent Gaussian potential is applied at the positive x-axis side.



$V=10\text{MeV}$



$V=30\text{MeV}$



$V=50\text{MeV}$

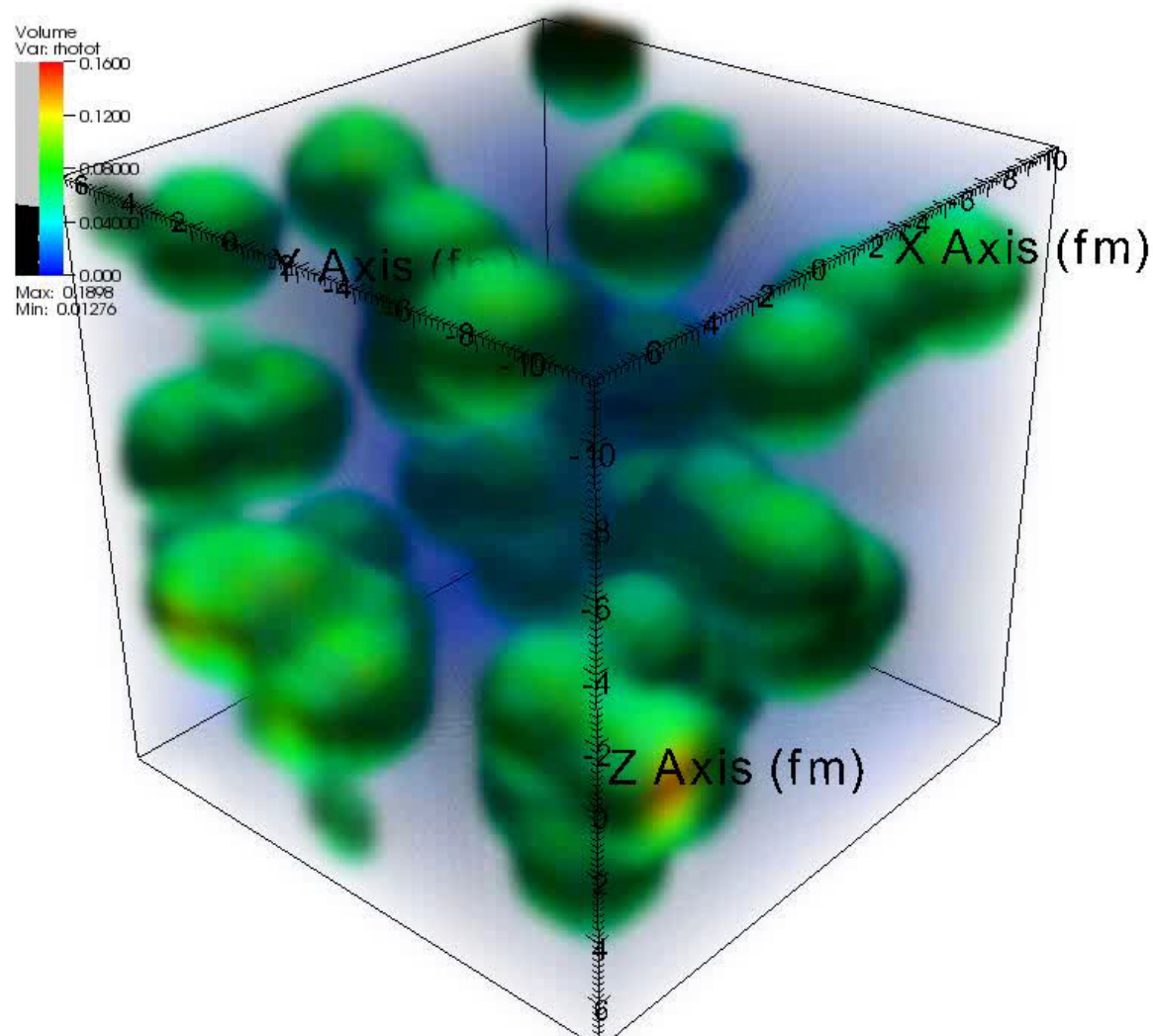
Summary

- Cluster structure is present in HF, but diminishes rapidly with A.
- Stability crucially dependent on symmetries
- The superdeformed chain-type states are unstable with respect to a bending deformation, but may be present as resonances.
For 4α they appear stabilized by rotation.
- TDHF shows both such resonances and a triangle-shape state as well as rotating chains
- There may be a new access to toroidal nuclei
- THDF dynamics leads to a nonlinear coupling of collective modes. Stability is not cleared up completely!
- Localization analysis appears attractive for clustering.

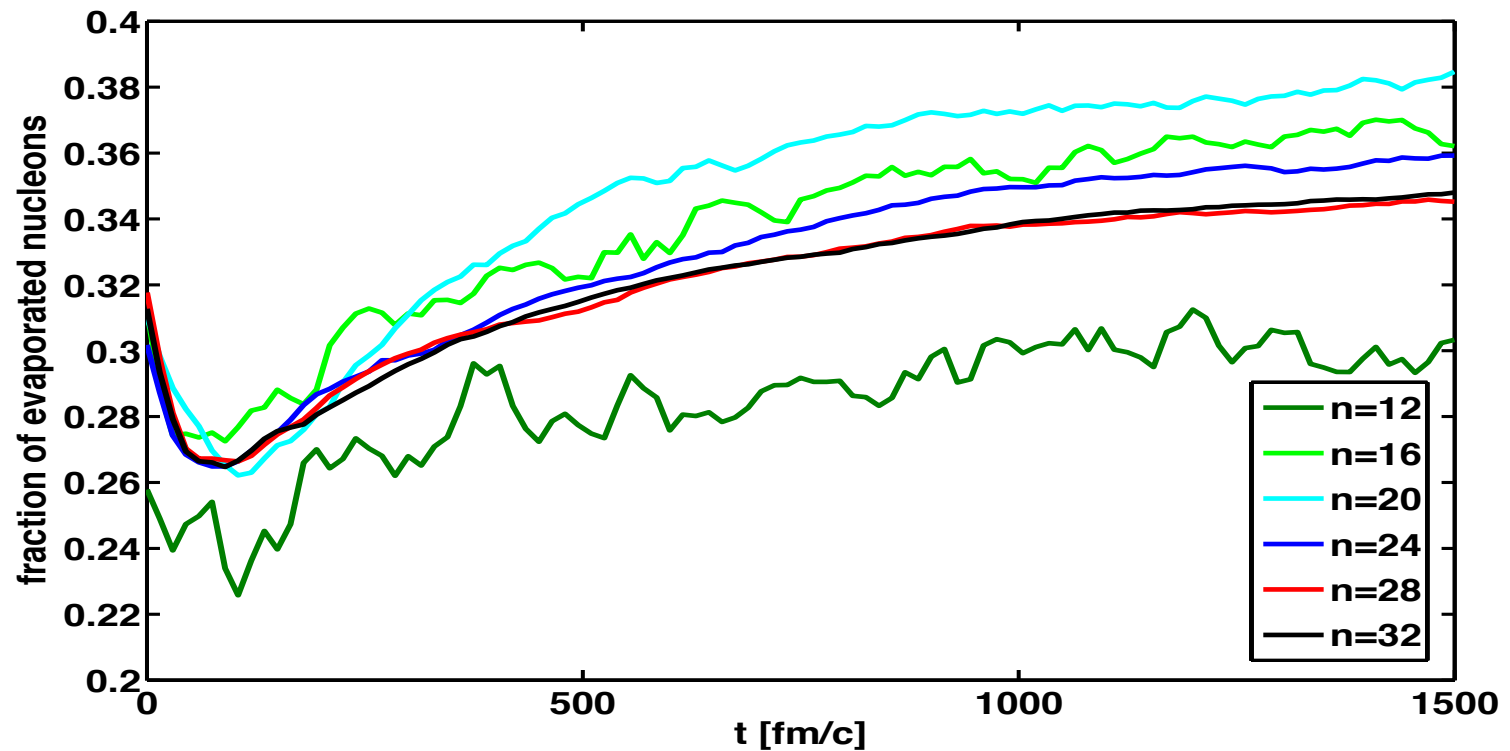
Astrophysics

- Principal investigators: B. Schuetrumpf, Kei Iida (Kochi), M. Klatt and K. Mecke (Erlangen).
- Simulation of the “pasta” phase of nuclear matter
- Periodic cubic box filled with α -particles
- Thermal excitation through initial velocities for the particles
- A relatively rapid thermalization is observed, leading to the different pasta structures depending on initial density and temperature

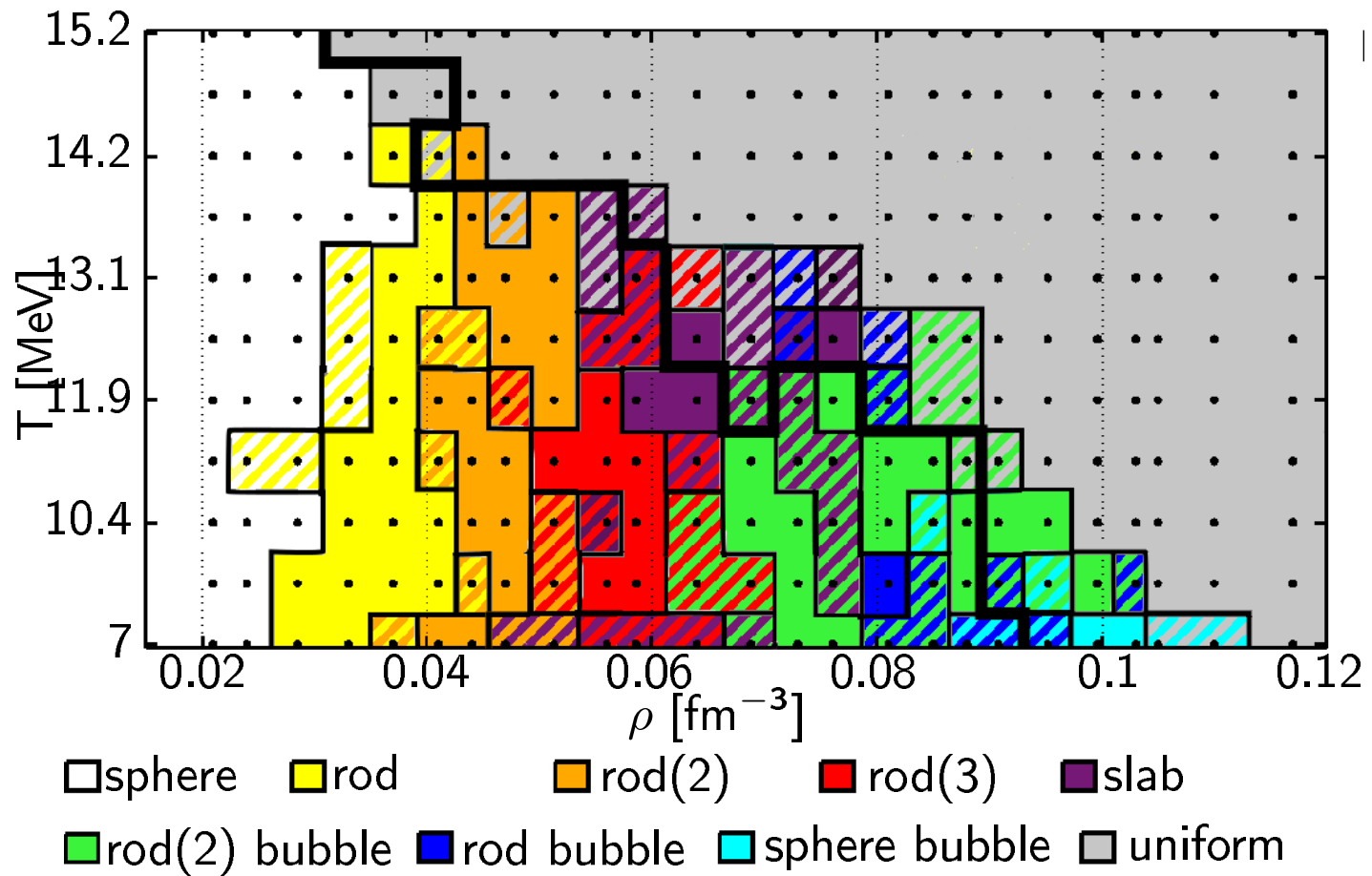
Thermalization

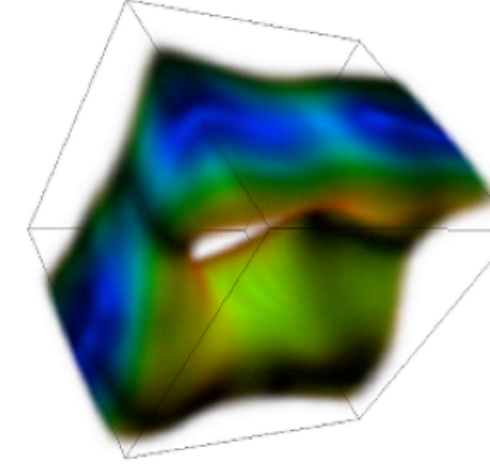
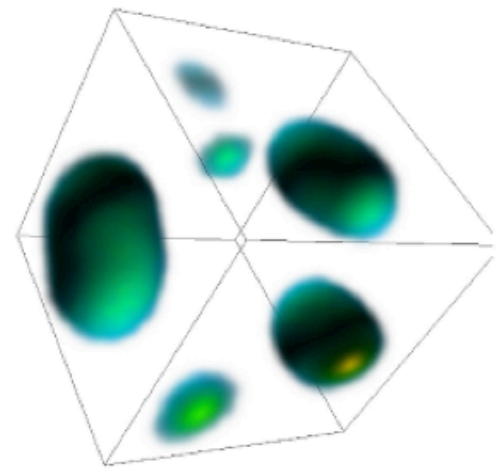
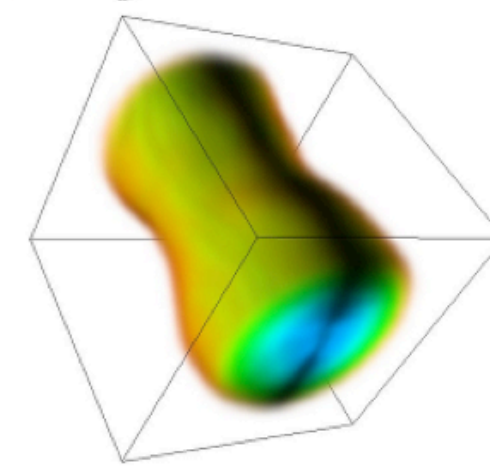
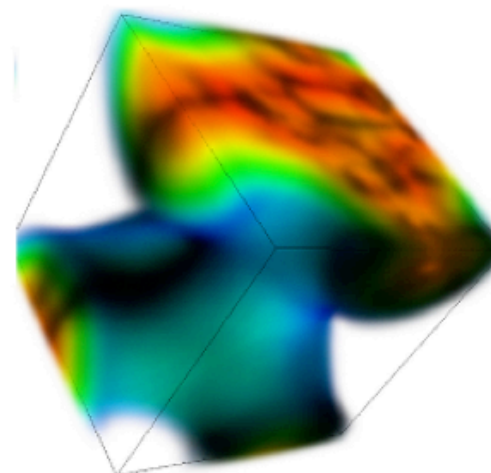
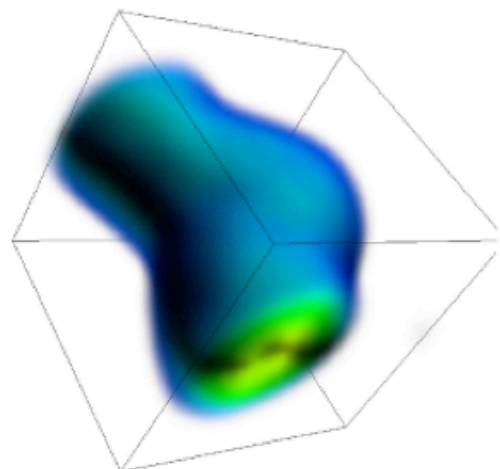
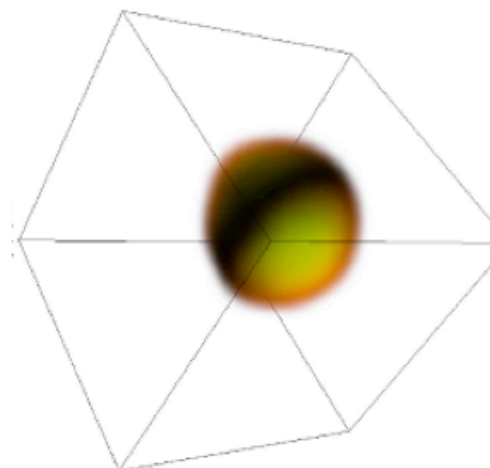
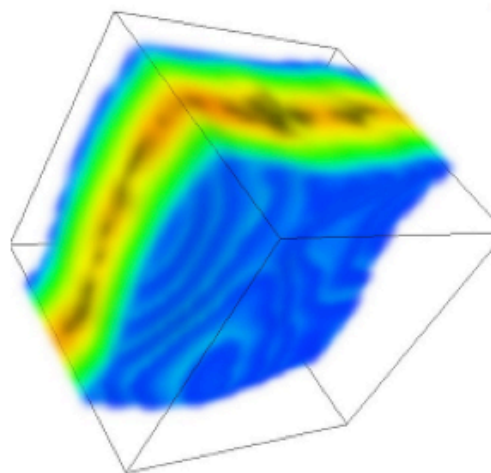
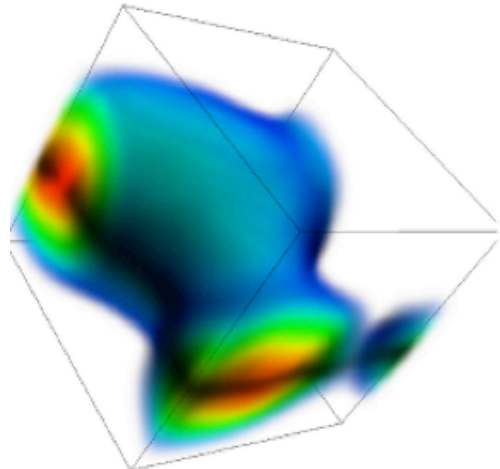


Equilibration



Phase diagram





Minkowski functional analysis

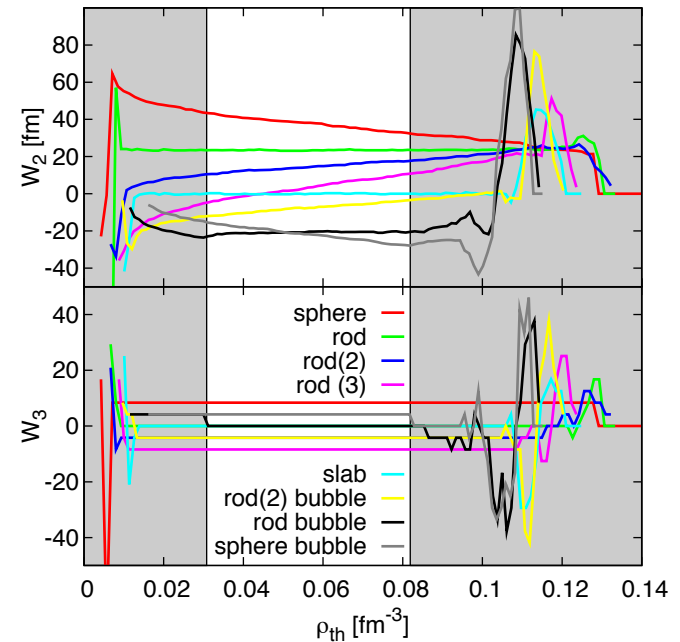
(with M. Klatt and K. Mecke
(University of Erlangen))

- b/w-picture $\begin{cases} \rho < \rho_{Th} & \rightarrow \text{white} \\ \rho > \rho_{Th} & \rightarrow \text{black} \end{cases}$

- 4 scalars to describe pictures:

- ① W_0 : Volume
- ② W_1 : Surface Area
- ③ W_2 : Integral Mean Curvature
- ④ W_3 : Euler Characteristic

(# of connected components - # of tunnels + # of cavities)
($W_3(\text{sphere})=2$, $W_3(\text{torus})=0$, $W_3(\text{double torus})=-2\dots$)



- physical values for ρ_{Th} are between $0.03 \frac{1}{\text{fm}^3}$ and $0.09 \frac{1}{\text{fm}^3}$

New shapes

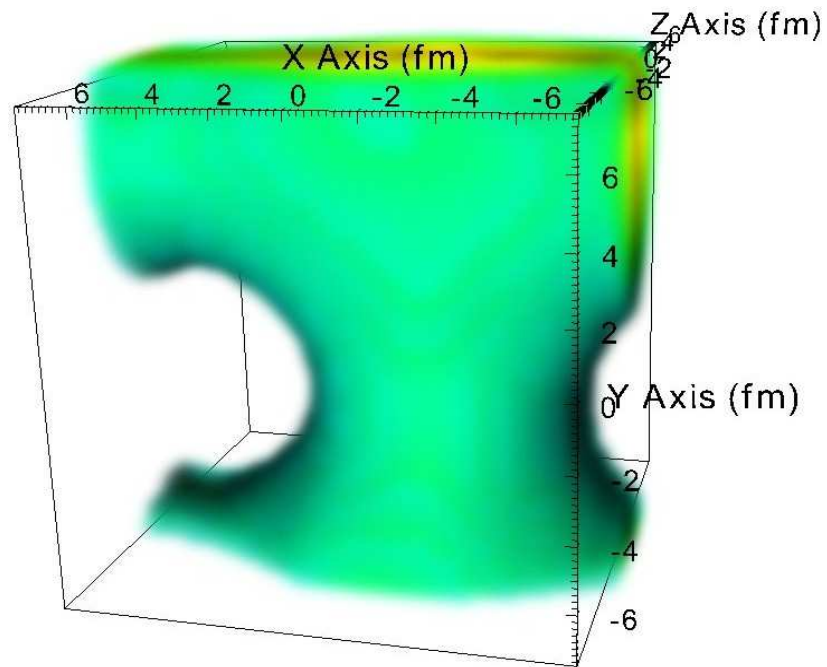


Figure: Rod(2)-Shape

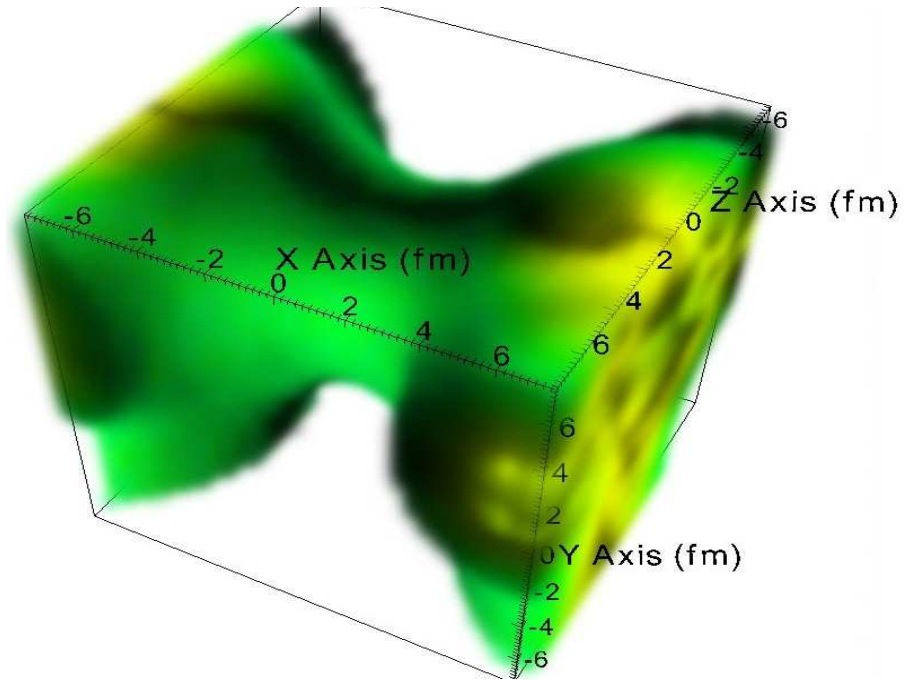
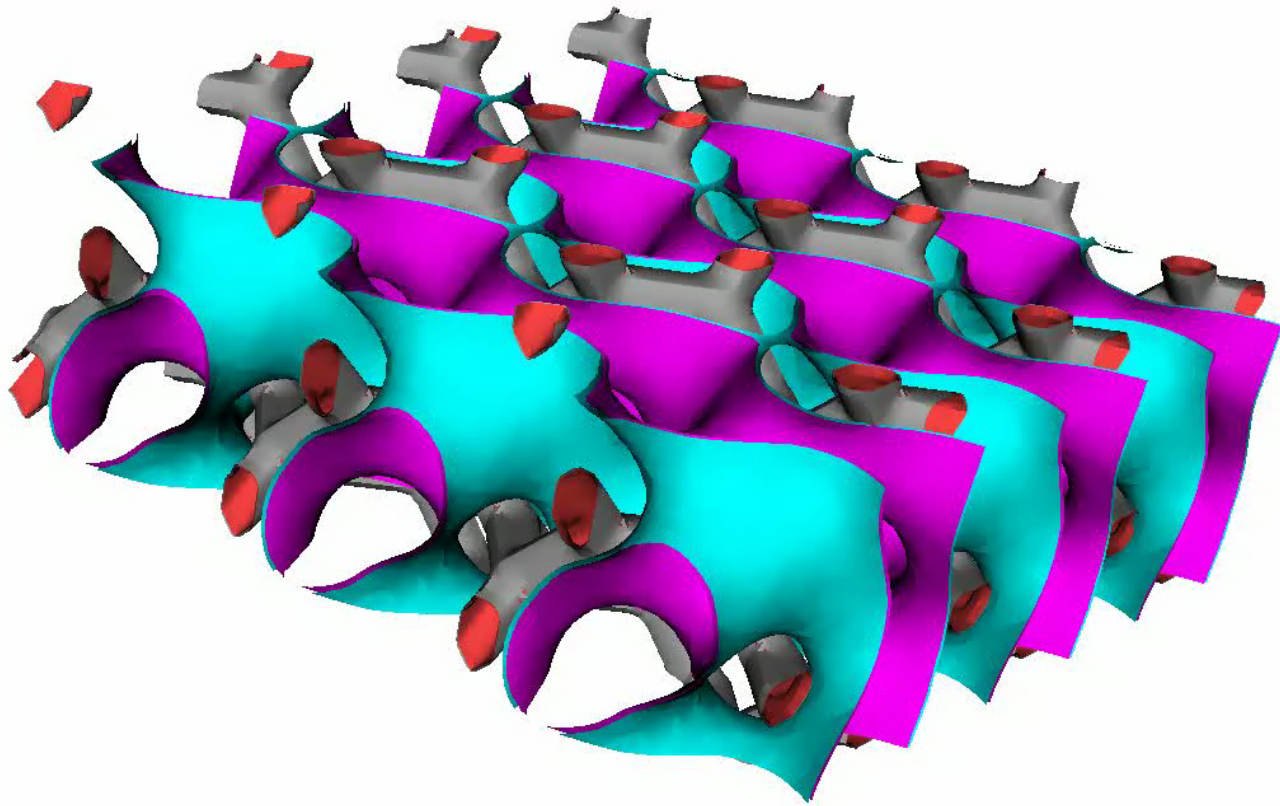


Figure: Rod(3)-Shape

Preliminary: gyroid structure



Wikipedia article

- A gyroid is a certain infinitely connected triply periodic minimal surface discovered by Alan Schoen in 1970.
- The gyroid has space group $Im\bar{3}d$. Channels run through the gyroid labyrinths in the (100) and (111) directions; passages emerge at 70.5 degree angles to any given channel as it is traversed, the direction at which they do so gyrating down the channel, giving rise to the name "gyroid".
- In 1986, Osserman proved that it contains no straight lines, in 1996 Große-Brauckmann and Wohlgemuth proved that it is embedded, in 1997 Große-Brauckmann proved that it has no reflectional symmetries.



Summary

- A chains could be stabilized by rotation
- Toroidal light nuclei show unusual quantization and could be linked to spaghetti
- A gas of α -particles rapidly settles into a pasta structure
- The full range of pasta formations was observed
- It is likely that even a gyroid structure was formed
- TDHF is not useful for detailed studies because of the computational expense, but might be applied to vibrations of the pasta structures
- The HF/TDHF code Oak3d will soon be available in source form